Quaternary Science Reviews 26 (2007) 894–919

Relative sea level changes and regional tectonic evolution of seven coastal areas in NW Greece since the mid-Holocene

Andreas Vött*

Faculty of Geography, Philipps-Universität Marburg, Deutschhausstr. 10, D-35032 Marburg/Lahn, Germany

Received 12 June 2006; received in revised form 17 January 2007; accepted 18 January 2007

Abstract

This study presents relative sea level (RSL) curves for seven coastal areas in Akarnania and the northwestern Peloponnese (NW Greece) since the mid-Holocene. RSL fluctuations are deduced from 48 ^{14}C-AMS dated sedimentological sea level markers from 27 vibracores drilled in near-coast geological archives as well as from six geoarchaeological sea level indicators of known ages. Seven palaeo sea level curves including uncertainty bands are reconstructed for a coastal zone spanning a distance of 150 km. Considerable intra-regional differences in sea level evolution exist. These differences are mainly due to tectonic reasons. In general, RSL in northwestern Greece has never been higher than today. Rates of local sea level rise were highest until 5500–5000 cal BC (up to 12.3 m/ka) and lowest during 4000–500 cal BC (0.2–1.4 m/ka). During the past 2500 or so years, RSL has accelerated anew (0.7–2.7 m/ka). Calculating differences between local mean sea level curves provides quantitative information on intra-regional differences of tectonic activity. The coastal plains of Palairos and Elis show signs of uplift, whereas the Mytikas and Boukka plains are strongly subsiding. Compared to other areas of the eastern Mediterranean, northwestern Greece has been subject to significant net long-term subsidence. Regional tectonic events (RTEs) were detected for the time around 4000, 2500, 500 and 250 cal BC as well as around 250 and 1250 cal AD. RTEs are characterized by changes of uplift/subsidence rates or by the redirection of local tectonic movements. The question if some of the RTEs were of a supra-regional nature is still open. From a geodynamic point of view, the results presented show that Akarnania's southwestern fringe is being downwarped while the tectonic block as a whole is moving towards the southwest. Strongest subsidence rates are observed for central Akarnania. At Akarnania's fringes, subsidence is reduced by the influence of strong uplift of adjacent areas such as around Preveza and the northern Peloponnese.
© 2007 Elsevier Ltd. All rights reserved.

1. Introduction

There have been several different approaches taken to reconstruct Holocene sea level fluctuations. Geological and geochronological studies conducted in areas which are predominantly characterized by tectonic stability or which are assumed to underlie constant rates of vertical movement are used to determine a global "eustatic" signal (cf. Stanley, 1995). The Barbados sea level curve (Fairbanks, 1989), for instance, has been applied to different areas all over the world, lately to the Ionian and Aegean Seas by Perissoratis and Conispoliatis (2003). Another approach to reconstruct sea level changes is based on glacio- and hydro-isostatic models which are used to calculate sea level stands for different time periods (Lambeck and Chappell, 2001; Peltier, 2002; Stocchi et al., 2005). However, they are difficult to apply to areas of strong tectonic activity (Pirazzoli, 1997). Therefore, over the last decade, a number of efforts have been made to combine these models with field data and to adapt them to a more regional scope, for instance by Lambeck et al. (2004) in Italy and Sivan et al. (2004) for the Mediterranean coast of Israel.

In this paper relative sea level (RSL) curves are presented for seven adjacent coastal areas in northwestern Greece based on sedimentological data from vibracores as well as on geomorphological and geoarchaeological indicators. The main objectives are (i) to document regional differences in sea level evolution, (ii) to attribute these differences to possible triggering factors, especially to tectonics, (iii) to detect local to regional tectonic patterns, their dynamics and dimensions and (iv) to

*Tel.: +49 6421 282 59 17; fax: +49 6421 282 89 50.
E-mail address: voett@staff.uni-marburg.de.

0277-3791/$ - see front matter © 2007 Elsevier Ltd. All rights reserved.
doi:10.1016/j.quascirev.2007.01.004

detect large-scale correlations between local sea level curves.

2. Geological and tectonic background

The study area consists of seven coastal zones in Akarnania and the northwestern Peloponnese, NW Greece, which together span a distance of 150 km (Fig. 1). The Boukka coastal plain is located at the southeastern shore of the Ambrakian Gulf. The coastal plains of Palairos, Mytikas and Astakos open towards the Ionian Sea at the western fringe of the Akarnanian block. In the Acheloos River delta — one of the largest deltas in the eastern Mediterranean — we examine RSL changes around the former Echinades Island of Trikardo and in the environs of the Lagoon of Etoliko. The coastal plains of Elis are located at the opposite side of the Gulf of Patras in the northwestern Peloponnese.

The study area belongs to the Ionian Zone of the Western Hellenic Nappe of the outer Hellenides. The stratigraphic sequence starts with basal Triassic evaporites, up to 3.5 km thick. Subsequently, a 3 km thick package of dolomites and limestones was formed on top of large carbonate platforms during Triassic to Tertiary times. Over the course of the Eocene, the environment changed into a deep oceanic trough where 2 km of clastic sediments of the Western Hellenic Flysch, mostly clay, silt and sand, were deposited. At the Akarnanian coast, the flysch unit is mostly made up of fine grained marly sediments (Jacobshagen, 1986, pp. 20ff.).

The multiple plate junction offshore of the Ionian Islands — where Africa, the Adriatic and the Aegean form different types of plate boundaries by collision, subduction, transform faulting and spreading — is the major controlling factor for the geological and tectonic evolution of Akarnania and the western Peloponnese (Fig. 2; Sachpazi et al., 2000, p. 303). Since the late Miocene, WNW trending

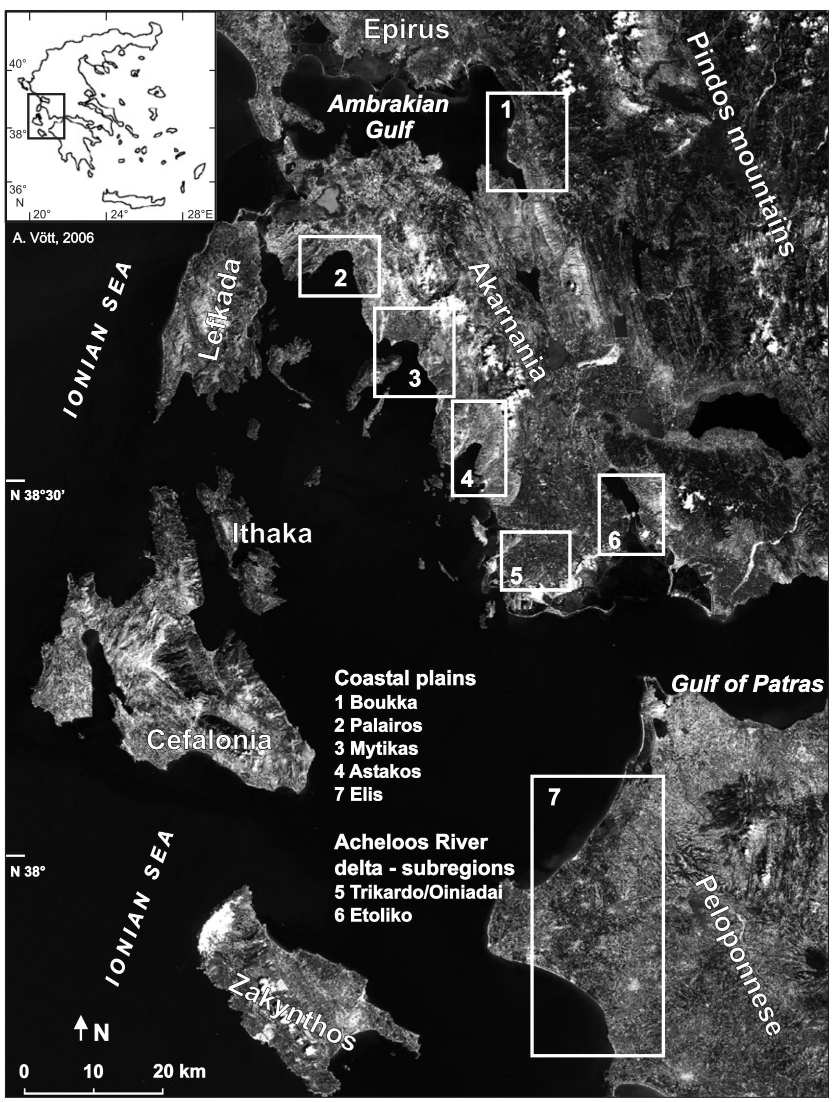

Fig. 1. Topographic overview of the Ambrakian Gulf, Akarnania, the Ionian Islands, and the northwestern Peloponnese (NW Greece). The white boxes mark the study areas. *Source of map*: Scenes from Landsat 7 ETM +, channels 3, 2, 1 (1999, 2000), assembled by M. May, 2006.

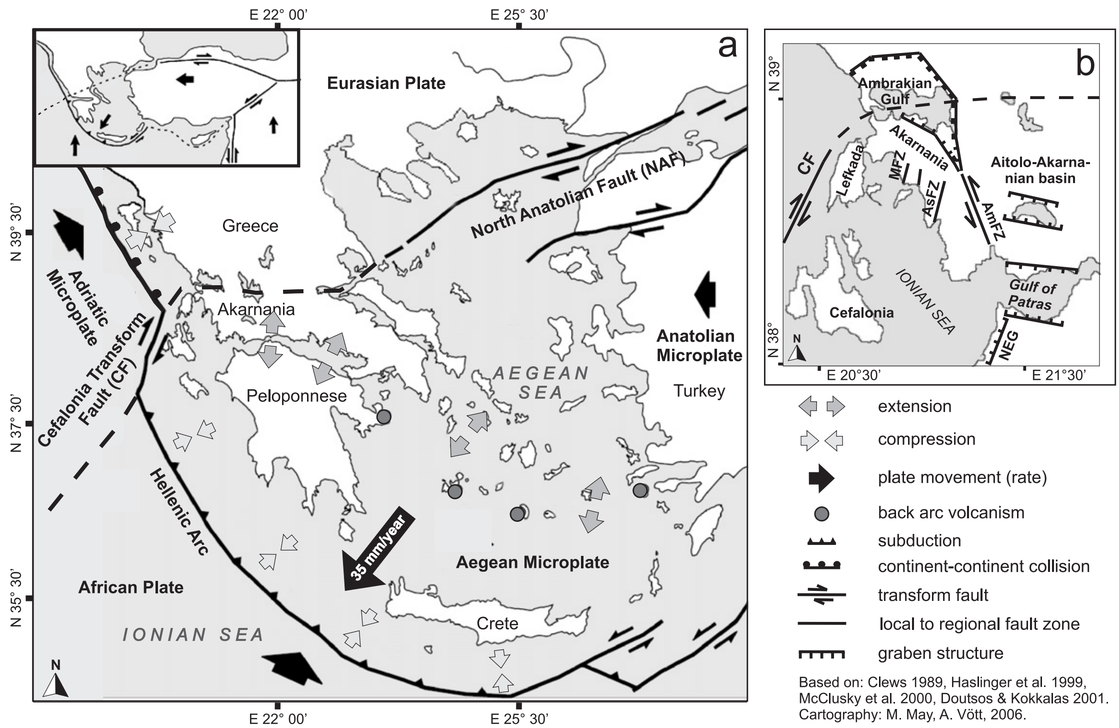

Fig. 2. Plate boundaries and geodynamic pattern of Greece and the Ionian and Aegean Seas. *Note*: CF—Cefalonia Transform Fault, AmFZ—Amfilochia Fault Zone, AsFZ—Astakos Fault Zone, MFZ—Mytikas Fault Zone, NEG—Northern Elis Graben.

graben structures such as the Corinthian and Ambrakian Gulfs as well as the Aitolo-Akarnanian Basin have been formed by pull-apart dynamics caused by the rapid movement of the Aegean microplate towards the SW (Papazachos and Kiratzi, 1996; Doutsos and Kokkalas, 2001). The right-lateral strike slip Cefalonia transform fault (CF) is responsible for the strong seismic activity in the area (Cocard et al., 1999; Louvari et al., 1999). Rates of crustal motion north and west of the CF are only 5 mm/a in western Greece, but east and south of the fault they reach 30 mm/a in the southern Peloponnese and 40 mm/a in Crete (Kahle et al., 1993, 1995; Cocard et al., 1999; McClusky et al., 2000). The Akarnanian block is separated from central Greece by the Amfilochia fault zone (AmFZ) (= Katouna fault zone; Fig. 2). The AmFZ thus represents an initial rifting stage with a left-lateral strike slip motion (Doutsos et al., 1987, p. 442; Clews, 1989, pp. 453f., Fig. 9; Haslinger et al., 1999, p. 202). Differential GPS measurements have shown that Akarnania is moving 5 mm/a faster towards the SW than its northern and western hinterland (Cocard et al., 1999, p. 45). Additionally, palaeomagnetic studies resulted in an average 40° clockwise rotation of northwestern Greece during 15–8 Ma and a second phase of 10° clockwise rotation after 4 Ma (van Hinsbergen et al., 2005, p. 30). Broadley et al. (2004) carried out palaeomagnetic analyses of Eocene limestones from northern Akarnania and found a large, up to 90° clockwise rotation of the Akarnanian block since Oligo-Miocene times. Both rifting and rotation dynamics are the triggering factors for the opening and spreading of the Ambrakian Gulf and the Gulf of Patras.

The Boukka coastal plain is part of the hanging wall of the NNW-SSE trending AmFZ. The area is characterized by active subsidence (King et al., 1997, p. 553f.). To the east, the Akarnanian-Amfilochian mountains are made up of thick sequences of the Western Hellenic Flysch unit.

The Palairos coastal plain is bounded by an active tectonic graben system. The western flank runs from NNE to SSW, the eastern flank from N to S. The westward movement of the Akarnanian mountains and the eastward migration of the Plaghia peninsula cause ongoing overthrusting of the central plain (Kontopoulos, 1990, Fig. 1). In the north of the plain, the swampy freshwater environment of Lake Voulkaria is located in a polje-like structure which evolved on top of almost horizontally lying Mesozoic bedrock units (Bousquet, 1976, Fig. 9).

The Mytikas graben structure was initiated by the subduction in the Hellenic Arc which began during Oligocene and early Miocene times. It is a product of NNE–SSW and NW–SE striking faults which separate Mesozoic rocks on the flanks from the Tertiary to Quaternary graben infill. Compression in a NW–SE direction since Tertiary times is responsible for active overthrusting and subsidence of the central basin (British Petroleum Co. Ltd., 1971, p. 53f.; Doutsos et al., 1987, pp. 436ff.; Clews, 1989).

The Astakos coastal plain shows a NNE–SSW trending tectonic half graben structure (Bousquet, 1976, Fig. 11) with its western flank uplifted along the Astakos fault zone (AsFZ; British Petroleum Co. Ltd., 1971, Fig. 9; IGME, 1986). There is ongoing overthrusting along the AsFZ in an easterly direction (Clews, 1989). The AsFZ is characterized by frequent earthquakes and mass movements along the fault scarp.

The rocky hills in the central Acheloos River delta, parts of the former Echinades Islands which were landlocked by alluvial sediments, are mostly made up of Triassic limestone and gypsum breccias. Bedrock is strongly karstified and represents a NNW–SSE running zone of tangential shearing and décollement during the Pindic orogeny in Miocene to early Pliocene times (British Petroleum Co. Ltd., 1971). The eastern delta shows Pliocene to Quaternary gypsum diapirism (Underhill, 1988). The Lagoon of Etoliko is part of the rift zone along the AmFZ which connects the Gulf of Patras and the Ambrakian Gulf. It thus represents a subsiding basin.

The coastal plains of Elis lie adjacent to the NNE–SSW trending northern Elis graben (NEG; IGME, 1977). The NEG represents the southern continuation of the Amfilochia–Katouna–Etoliko rift zone. Coral deposits found up to about 500 m above mean sea level (m a.s.l.) indicate that the eastern NEG footwall has been uplifted during the Quaternary (Stamatopoulos et al., 1988, 1994). The graben has been subsiding since Miocene times (Kelletat et al., 1976, pp. 456ff.; Kowalczyk and Winter, 1979, p. 327; Lekkas et al., 2000, p. 22). However, the promontory of the Chlemoutsi headland is a product of local gypsum diapirism related to thick basal Triassic evaporites. It represents a zone of strong local halokinetic uplift (Underhill, 1988; Maroukian et al., 2000).

3. Materials and methods

Sea level studies in northwestern Greece were carried out within the framework of palaeogeographical–geoarchaeological investigations of Holocene coastal changes. Between 2001 and 2005, 118 vibracores were drilled in near-coast geological archives (Vött et al., 2004; Brockmüller et al., 2005; Vött and Brückner, 2006; Vött et al., 2006a–c; Vött et al., in press a, b). Vibracoring was completed using an Atlas Copco corer with core diameters of 5 or 6 cm. The maximum recovery depth was 22 m. The position and the elevation of each coring site were measured by means of a differential GPS (type Leica SR 530).

Vertical and lateral facies variations were reconstructed using sedimentological, macro- and microfaunal and geochemical analyses of sediment samples. Multivariate geostatistics also proved a valuable tool for the determination of facies (Vött et al., 2002, 2003). We developed a geochronology of coastal changes using a set of 124 ^{14}C-AMS dates on organic material, mostly peat or plant remains and biochemically produced marine carbonate, preferably articulated specimens of molluscs. Marine samples were corrected for an average marine reservoir effect of 402 years (cf. Siani et al., 2000; Reimer and McCormac, 2002) although it has to be assumed that the real (palaeo) reservoir effect — still unknown — varies widely in different marine environments, such as lagoons, coastal swamps or littoral zones. In some cases, diagnostic ceramic fragments found in vibracores could be used for relative age determination.

The analyses presented in this paper are based on a selection of 27 vibracores that contain the most reliable ^{14}C-AMS dated sea level indicators encountered in the study area (Table 1). The closer geochronological framework results from (i) a pool of 61 ^{14}C-AMS dates (Table 1) from which 48 dates were finally chosen as valuable sedimentological sea level indicators (Table 2) and (ii) a further six dated archaeological structures that showed a clear relation to the palaeo sea level at the time when they were in use. All dates presented are calibrated ages in cal BC/AD or cal BP (Tables 1 and 2). Calibration was achieved using the calibration software Calib from Stuiver et al. (2006).

4. Relative sea level curves based on sedimentological and geoarchaeological indicators

The reconstruction of RSL changes is mainly based on sedimentological palaeo sea level markers. Peat from paralic swamps is considered to be one of the most reliable sea level indicators (Pirazzoli, 1991, p. 15). It accumulates where surface water discharge into the sea is retarded by beach ridges or levees or in lagoonal environments. A RSL rise is assumed to be balanced by increasing peat formation, with RSL fall resulting in peat weathering. Abrupt marine incursions, however, erode and disturb coastal peat layers. At the time of peat formation, sea level was slightly lower than sampling depth (see below). In cases where peat samples were not available, wood fragments, plant remains or shells of marine organisms were used as sea level indicators. Every dated sample was evaluated against the sedimentological and geomorphological background. Realistic estimations of the height of the water column during the time of deposition were based on observations of modern sedimentary environments. When dating shells of marine macrofauna, articulated specimens were preferred in order to minimize the risk of reworking effects. Moreover, it was checked if δ^{13}C-values differ from values given in literature (cf. Geyh, 2005, p. 72). If differences were too large, the ^{14}C-AMS dated sample was considered as unreliable and excluded from further interpretation. In case of an age inversion within a geochronological sequence, stratigraphic comparisons with adjacent vibracore profiles were used to detect unreliable samples which were then taken out of the data set.

Table 2 specifies the general quality and the uncertainty margins of each sample used as sedimentological sea level marker. In cases of peat samples from coastal swamps, palaeo sea level is assumed to be within a band of 50 cm below sampling depth. This value is derived from many GPS measurements in coastal Akarnania where peat formation and groundwater level is directly influenced by modern sea level (see also Pirazzoli, 1996, p. 48; Behre,

Table 1
Radiocarbon dating results for selected samples from coastal Akarnania and the northwestern Peloponnese

Samples			Coring site		^{14}C-AMS results				
Sample name	Depth (m b.s.)	Depth (m b.s.l.)	Position latitude (N)/ longitude (E)	Elevation (m a.s.l.)	Lab. No. (UtC)	δ^{13}C (ppm)	^{14}C Age (BP)	1σ max; min (cal BP)	1σ max; min (cal BC)
AST 1/6	5.32	3.33	38° 32.6168′/21° 05.6765′	1.99	11555	−24.8	5811±47	6716; 6550	4766; 4600
AST 1/11	9.80	7.81	38° 32.6168′/21° 05.6765′	1.99	11556	−25.7	6212±49	7224; 7021	5274; 5071
AST 1/13	10.88	8.89	38° 32.6168′/21° 05.6765′	1.99	11557	−27.4	6220±50	7229; 7025	5279; 5075
AST 2/9 PR	2.93	2.83	38° 32.1030′/21° 05.6356′	0.10	12297	−28.0	2574±37	2756; 2547	806; 597
AST 2/23 PR	6.50	6.40	38° 32.1030′/21° 05.6356′	0.10	12296	−12.6	5597±47	6406–6312	4456–4362
AST 2/32 M	9.80	9.70	38° 32.1030′/21° 05.6356′	0.10	12295	−0.5	6887±42	7429–7358	5479–5408*
AST 4/36 HK	14.80	7.42	38° 32.9038′/21° 06.0714′	7.38	12299	−26.3	7420±50	8323; 8178	6373; 6228
AST 4/42 HK	17.10	9.72	38° 32.9038′/21° 06.0714′	7.38	12298	−31.0	7313±48	8168; 8041	6218; 6091
BOU 1/14 PR	5.33	4.54	38° 55.0967′/21° 08.9800′	0.79	12301	−27.9	2427±40	2700; 2358	750; 408
BOU 1/19 M	9.74	8.95	38° 55.0967′/21° 08.9800′	0.79	12300	−3.0	5407±46	5843–5726	3893–3776*
BOU 3/27+PR	14.41	11.96	38° 56.2817′/21° 08.9983′	2.45	12302	−28.4	6140±50	7154; 6910	5204; 4960
BOU 4/13 PR	5.60	5.55	38° 57.4700′/21° 08.9267′	0.05	12305	−27.5	5368±49	6271; 6003	4321; 4053
BOU 4/19+PR	7.64	7.59	38° 57.4700′/21° 08.9267′	0.05	12304	−27.8	4164±47	4821; 4620	2871; 2670
BOU 4/27 M	11.65	11.60	38° 57.4700′/21° 08.9267′	0.05	12303	−3.6	5940±60	6396–6289	4446–4339*
BOU 5/13 M	4.53	3.84	38° 58.0917′/21° 09.1500′	0.69	13193	−4.4	2919±36	2738–2690	788–740*
BOU 5/17+PR	5.60	4.91	38° 58.0917′/21° 09.1500′	0.69	13681	−25.5	3034±34	3329; 3210	1379; 1260
BOU 5/27+PR	10.76	10.07	38° 58.0917′/21° 09.1500′	0.69	13680	−27.7	3150±33	3437; 3349	1487; 1399
BOU 7/18+M	6.65	6.41	38° 58.2483′/21° 09.6783′	0.24	13194	−3.5	5608±49	6047–5920	4097–3970*
ELI 4/16 M	6.32	4.20	37° 55.3400′/21° 12.0833′	*2.12*	13682	0.0	5583±39	6009–5906	4059–3956*
ELI 5/15+PR	8.72	3.73	37° 50.2700′/21° 13.4450′	4.99	13685	−28.1	5002±44	5859; 5658	3909; 3708
ELI 5/19+PR	9.82	4.83	37° 50.2700′/21° 13.4450′	4.99	13684	−27.5	6153±40	7156; 6996	5206; 5046
ELI 9/13 PR	5.56	3.83	38° 05.0250′/21° 21.8150′	1.73	13688	−25.2	6860±44	7740; 7625	5790; 5675
ELI 10/9+PR	3.63	3.73	38° 06.0517′/21° 20.9800′	−0.10	13689	−13.2	2613±47	2346; 2210	396–260*
MYT 1/6	3.78	1.57	38° 40.5879′/20° 57.2572′	2.21	11558	−7.9	5439±48	6288; 6197	4338; 4247
MYT 3/10 PR	3.72	2.29	38° 40.4850′/20° 56.5983′	1.43	12308	−28.4	1758±44	1719–1603	231–347 AD
MYT 3/18 PR	6.46	5.03	38° 40.4850′/20° 56.5983′	1.43	12307	−27.8	3399±48	3695–3572	1745–1622
MYT 3/26+PR	12.76	11.33	38° 40.4850′/20° 56.5983′	1.43	12306	−28.9	6610±50	7560; 7436	5610; 5486
MYT 8/10+M	5.78	4.60	38° 40.3917′/20° 57.6833′	1.18	13195	0.9	2827±38	2676–2529	726–579*
MYT 8/15 PR	8.75	7.57	38° 40.3917′/20° 57.6833′	1.18	13196	−24.6	5340±41	6193; 5999	4243; 4049
MYT 8/19+PR	10.56	9.38	38° 40.3917′/20° 57.6833′	1.18	13197	−28.8	6177±42	7175; 7003	5225; 5053
MYT 10/26+PR	13.50	12.10	38° 40.4350′/20° 56.7767′	1.40	13198	−28.8	6997±48	7921; 7755	5971; 5805
OIN 1/4	1.83	1.35	38° 28.2783′/21° 11.0199′	0.48	11559	−26.6	1642±41	1422; 1606	344; 528 AD
OIN 4/2 PR	0.66	1.77	38° 26.3650′/21° 08.8283′	−1.11	12311	−27.5	748±36	698–658	1252–1292 AD
OIN 6/6 PR	1.80	1.40	38° 29.0533′/21° 10.3817′	0.40	12316	−27.8	1469±38	1383–1318	567–632 AD
OIN 31/9+PR	4.27	3.45	38° 26.6267′/21° 18.0135′	0.82	13200	−26.3	4042±43	4569; 4423	2619; 2473
OIN 31/14+PR	8.66	7.84	38° 26.6267′/21° 18.0135′	0.82	13201	−27.8	5874±49	6747–6640	4797–4690
OIN 31/16+PR	9.92	9.10	38° 26.6267′/21° 18.0135′	0.82	13202	−29.0	6580±46	7552; 7430	5602; 5480
OIN 35/23+PR	12.44	12.36	38° 27.2233′/21° 21.8717′	0.08	13207	−27.8	7330±50	8176; 8042	6226; 6092
OIN 44/17 PR	6.90	4.10	38° 23.9583′/21° 12.0610′	2.80	13701	−28.3	4232±42	4852; 4663	2902; 2713
OIN 44/20+PR	7.63	4.83	38° 23.9583′/21° 12.0610′	2.80	13700	−28.9	4399±40	5038; 4876	3088; 2926
OIN 44/28 PR	11.36	8.56	38° 23.9583′/21° 12.0610′	2.80	13699	−27.7	6393±39	7415; 7272	5465; 5322
OIN 49/7+PR	2.58	1.95	38° 24.3433′/21° 11.4467′	0.63	13709	−28.5	570±38	633; 537	1317; 1413 AD
OIN 49/9+PR	3.70	3.07	38° 24.3433′/21° 11.4467′	0.63	13708	−28.0	2107±41	2130; 2005	180; 55
OIN 49/15+PR	5.28	4.65	38° 24.3433′/21° 11.4467′	0.63	13707	−31.7	4413±49	5211; 4875	3261; 2925
OIN 49/19+GPRA	6.68	6.05	38° 24.3433′/21° 11.4467′	0.63	13706	−27.5	5730±50	6616; 6451	4666; 4501
OIN 49/20+PR	7.71	7.08	38° 24.3433′/21° 11.4467′	0.63	13705	−28.3	6160±50	7156; 7002	5206; 5052
OIN 55/4+PR	1.85	1.05	38° 24.4100′/21° 11.3167′	0.80	13715	−28.2	435±38	522–475	1428–1475 AD
OIN 55/16+PR	5.89	5.09	38° 24.4100′/21° 11.3167′	0.80	13714	−20.6	5542±48	6396; 6294	4446; 4344
OIN 63/15+PR	6.57	5.34	38° 24.2936′/21° 11.4346′	1.23	Erl 9057	−28.2	5144±50	5985; 5761	4036; 3812
PAL 2/3	1.75	1.41	38° 48.0431′/20° 51.6742′	*0.34*	11564	−9.9	3675±48	4086; 3927	2136; 1977
PAL 2/6	3.95	3.61	38° 48.0431′/20° 51.6742′	*0.34*	11565	−2.2	5085±42	5903; 5752	3953; 3802*
PAL 2/7	4.33	3.99	38° 48.0431′/20° 51.6742′	*0.34*	11578	−1.4	5326±41	6176; 5997	4226; 4047*
PAL 2/10	5.77	5.43	38° 48.0431′/20° 51.6742′	*0.34*	11579	−0.8	6096±41	7005–6887	5055–4937*
PAL 2/11	6.35	6.01	38° 48.0431′/20° 51.6742′	*0.34*	11580	−5.1	5958±46	6401–6308	4451–4358*
PAL 2/14	7.85	7.51	38° 48.0431′/20° 51.6742′	*0.34*	11581	−2.1	6644±46	7569–7484	5619–5534*
PAL 2/15	8.20	7.86	38° 48.0431′/20° 51.6742′	*0.34*	11582	1.3	6780±50	7660–7590	5710–5640*
PAL 2/17	8.85	8.51	38° 48.0431′/20° 51.6742′	*0.34*	11583	−3.7	6048±43	6944; 6800	4994; 4850*
PAL 2/21	10.58	10.24	38° 48.0431′/20° 51.6742′	*0.34*	11211	−1.4	7345±40	7836–7746	5886–5796*
PAL 2/26	12.29	11.95	38° 48.0431′/20° 51.6742′	*0.34*	11584	−28.9	7192±47	8101; 7949	6151; 5999

Table 1 (*continued*)

Samples			Coring site		^{14}C-AMS results				
Sample name	Depth (m b.s.)	Depth (m b.s.l.)	Position latitude (N)/ longitude (E)	Elevation (m a.s.l.)	Lab. No. (UtC)	δ^{13}C (ppm)	^{14}C Age (BP)	1σ max; min (cal BP)	1σ max; min (cal BC)
PAL 8/11	5.08	4.52	38° 47.9833′/20° 51.2950′	0.56	12334	−27.5	5568±47	6398; 6307	4448; 4357
PAL 8/22 PR	10.42	9.86	38° 47.9833′/20° 51.2950′	0.56	12333	−27.3	7061±43	7937; 7837	5987; 5887
P 11#	7.70	3.50	~37° 49.50′/~21° 15.00′	4.20	UCR 1253	Unknown	6300±135	7414; 7022	5465; 5073
P 15#	2.50	2.00	~38° 00.00′/~21° 18.30′	0.50	UCR 1243	Unknown	2835±75	3063–2858	1114–909

Note: a.s.l.—above sea level; b.s.—below ground surface; b.s.l.—below sea level; *—marine reservoir correction with 402 years of reservoir age; 1σ max; min cal BP/BC (AD)—calibrated ages, 1σ-range; ";"—there are several possible age intervals because of multiple intersections with the calibration curve; Lab. No.—laboratory number, University of Utrecht (UtC), University of California Riverside (UCR), University of Erlangen-Nürnberg (Erl); #—radiocarbon dates published by Kraft et al. (2005), recalibrated. The table also contains dates which were not considered for further interpretation of palaeo sea level due to missing reliability (see Figs. 3–5, 7–8, 10–12 and text for further explanation).

2003, p. 16). If the dated peat unit was taken from a thin peat layer (<10 cm) which intersects thick packages of mineral deposits, the uncertainty width of the palaeo sea level band was reduced to 25 cm. Using wood fragments, plant remains or marine shells, palaeo sea level bands were deduced from the sedimentary environment, the stratigraphic sequence as a whole as well as from water depth measurements in comparable recent ecosystems. Samples from (sub-) littoral environments were used to define a palaeo sea level band of 100 cm above or around sampling depth depending on the sedimentary context. Concerning samples embedded in a lagoonal facies, palaeo water level was also considered to be at most 100 cm above sampling depth. This corresponds to recent observations of maximum lagoonal water depths along the Akarnanian coast between the Katafourkou Lagoon in the coastal plain of Boukka and the lagoons of the Acheloos River delta. In cases where thin layers of lagoonal mud directly cover bedrock units and thus represent a transgressive situation, palaeo water level was assumed not to have been higher than 50 cm above sampling depth. Marine shells from back beach environments indicate that palaeo mean sea level was close to sampling depth; however, samples may have been deposited both below mean sea level in swampy back beach depressions and above mean sea level in the distal part of alluvial fans bordering the beach ridge. Based on measurements in modern environments, the margins of the palaeo mean sea level band were thus assumed to lie 100 cm below and 50 cm above sampling depth. Samples from limnic deposits were only used, if the core stratigraphy documents temporary saltwater inflow into the coastal lake environment.

The quality of sedimentological sea level indicators is strongly influenced by the degree of post-depositional sediment compaction and displacement. Mechanical compaction is controlled by the predominant grain size of the sediment, by its organic and water content, and by the thickness of the overlying deposits. High variability of these factors in natural systems make it difficult to almost impossible to find realistic models of how the porosity of a sediment stack decreases with depth and time (Einsele, 2000, p. 653). However, the higher the proportion of coarse grains such as sand and gravel, the lower the compaction of mineral deposits. In terms of palaeo sea level research, compaction of purely sandy deposits is almost negligible whereas compaction of organic sediments such as peat may reach 90% by volume (Shennan and Horton, 2002, p. 512). Where peat compaction and peat weathering are strong, they can even become of major influence to ongoing coastal evolution (Long et al., 2006).

Based on stratigraphic comparisons, and in the absence of sound geotechnical corrections, it was assumed that compaction of mineral deposits in coastal Akarnania is low and spatially uniform in the seven areas under study (see Sections 4.3 and 4.5.1). Peat compaction was assumed to be negligible in cases of thin peat layers and peat samples from basal peat units overlying early to mid-Holocene mineral deposits (cf. Brunetti et al., 1998, p. 34; Gehrels, 1999). Generally, peat samples were taken from the basal part of a peat unit. In cases where peat samples were taken from the upper part of a peat unit or if compaction of lower peat units had to be taken into account, peat compaction was estimated as 50–100 cm (Table 2). Illustrative stratigraphic profiles are presented for selected vibracore profiles from the Mytikas coastal plain (Fig. 6) and the central Acheloos River delta around Trikardo (Fig. 9). Stratigraphic sequences from other coastal sites are presented by Brockmüller et al. (2005), Vött et al. (2006a–c), Vött et al. (in press a, b) and Vött (in press).

Submerged archaeological remains along the coast of the study area mostly date to Classical-Hellenistic to Roman times (Murray, 1982). They were regarded as reliable sea level indicators if (i) the structures can be clearly identified and the type of the building is known, (ii) their age is documented by ceramic findings and (iii) there is a distinct relation to the palaeo sea level, as is the case for harbour installations such as jetties (cf. Vött and Brückner, 2006).

Table 2
Radiocarbon dated palaeo sea level markers from northwestern Greece

Samples			Reconstruction of palaeo sea level band			Sedimentary context	Calibrated ages	
Sample name	Sample description	Depth (m b.s.l.)	Upper Limit (cm)	Lower limit (cm)	Palaeo mean sea level (m b.s.l.)		1σ max; min (cal BP)	1σ max; min (cal BC)
AST 1/13	Wood fragment	8.89	+100	±0	8.39	(transitional lake to) lagoon	7229; 7025	5279; 5075
AST 2/9 PR	Wood fragment	2.83	+100	±0	2.33	Shallow marine, (sub-)littoral	2756; 2547	806; 597
AST 2/32 M	*T. planata,* articulated specimen	9.70	+100	±0	9.20	Shallow marine, (sub-)littoral	7429–7358	5479–5408*
AST 4/42 HK	Charcoal	9.72	−180	−380	12.52	Limnic environment, estimation based on stratigraphic comparison	8168; 8041	6218; 6091
BOU 1/14 PR	Unidentified plant remain	4.54	+100	±0	4.04	Lagoon	2700; 2358	750; 408
BOU 3/27++PR	Unidentified plant remain	11.96	+100	−50	11.71	Transitional lagoon to lake, deposits include remains of *Phragmites* sp.	7154; 6910	5204; 4960
BOU 4/19+PR	Enriched organic material	7.59	+100	±0	7.09	Shallow marine, (sub-)littoral	4821; 4620	2871; 2670
BOU 4/27 M	*C. glaucum,* articulated specimen	11.60	+100	±0	11.10	Lagoon	6396–6289	4446–4339*
BOU 5/13 M	*C. glaucum*, articulated specimen	3.84	+100	±0	3.34	Lagoon	2738–2690	788–740*
BOU 5/17+PR	Plant remains, peat-like	4.91	±0	−25	5.03	Paralic swamp, thin peat layer (5 cm thick)	3329; 3210	1379; 1260
ELI 4/16 M	*D. exoleta*, articulated specimen	4.20	+100	±0	3.70	Lagoon	6009–5906	4059–3956*
ELI 5/15+PR	Peat, organic material	3.73	±0	−50	3.98	Paralic swamp, thin peat layer	5859; 5658	3909; 3708
ELI 5/19+PR	Peat, organic material	4.83	±0	−50	5.08	Paralic swamp, sample from base of peat layer	7156; 6996	5206; 5046
ELI 9/13 PR	Unidentified plant remain	3.83	+25	±0	3.70	Transitional shallow marine (sublittoral) to supralittoral, swamp-like	7740; 7625	5790; 5675
ELI 10/9+PR	Sea weed remains	3.73	+200	+50	2.48	Shallow marine, (sub-) littoral, mat of sea weed	2346; 2210	396–260*
MYT 3/10 PR	Peat, organic material	2.29	+50	−50	2.29	Paralic swamp, sample from base of peat layer, peat compaction	1719–1603	231–347 AD
MYT 3/18 PR	Peat, organic material	5.03	+50	−50	5.03	Paralic swamp, sample from base of peat layer, peat compaction	3695–3572	1745–1622
MYT 3/26+PR	Peat, organic material	11.33	±0	−50	11.58	Paralic swamp, thin basal peat layer	7560; 7436	5610; 5486
MYT 8/10+M	*D. exoleta*, articulated specimen	4.60	+100	±0	4.10	Shallow marine, transitional littoral to sublittoral	2676–2529	726–579*
MYT 8/15 PR	Unidentified plant remains	7.57	±0	−50	7.82	Shallow coastal lake, layers of plant fragments	6193; 5999	4243; 4049
MYT 8/19+PR	Peat, organic material	9.38	±0	−50	9.63	Paralic swamp, sample from base of peat layer	7175; 7003	5225; 5053
MYT 10/26+PR	Peat, organic material	12.10	±0	−50	12.35	Paralic swamp, thin basal peat layer	7921; 7755	5971; 5805
OIN 4/2 PR	Peat, organic material	1.77	+50	−50	1.77	Paralic swamp, thin peat layer, sediment compaction due to groundwater lowering	698–658	1252–1292 AD
OIN 31/9+PR	Peat, organic material	3.45	+50	−50	3.45	Paralic swamp, sample from base of peat layer, compaction of lower peat units	4569; 4423	2619; 2473
OIN 31/14+PR	Peat, organic material	7.84	+50	−50	7.84	Paralic swamp, affected by peat compaction	6747–6640	4797–4690

OIN 31/16 + PR	Peat, organic material	9.10	±0	−50	9.35	Paralic swamp, sample from base of peat layer	7552; 7430	5602; 5480
OIN 35/23 + PR	Peat, organic material	12.36	±0	−50	12.61	Paralic swamp, thin basal peat layer	8176; 8042	6226; 6092
OIN 44/17 PR	Peat, wood fragments	4.10	+50	−50	4.10	Paralic swamp, affected by peat compaction	4852; 4663	2902; 2713
OIN 44/20 + PR	Peat, organic material	4.83	±0	−50	5.08	Paralic swamp, sample from base of peat layer	5038; 4876	3088; 2926
OIN 44/28 PR	Wood fragment	8.56	+50	±0	8.06	Lagoon, transgressive sequence	7415; 7272	5465; 5322
OIN 49/7 + PR	Peat, organic material	1.95	+100	−50	1.70	Swamp, compaction of lower peat units	633; 537	1317; 1413 AD
OIN 49/9 + PR	Peat, organic material	3.07	+50	−50	3.07	Swamp, sample from base of peat layer, compaction of lower peat units	2130; 2005	180; 55
OIN 49/15 + PR	Peat, organic material	4.65	+50	−50	4.65	Swamp, thin peat layer, compaction of lower peat units	5211; 4875	3261; 2925
OIN 49/19 + GPRA	Peat, organic material	6.05	±0	−50	6.30	Swamp, sample from base of peat layer	6616; 6451	4666; 4501
OIN 49/20 + PR	Peat, organic material	7.08	±0	−50	7.33	Swamp, thin basal peat layer	7156; 7002	5206; 5052
OIN 55/4 + PR	Peat, wood fragment	1.05	±0	−50	1.30	Paralic swamp, thin peat layer	522–475	1428–1475 AD
OIN 63/15 + PR	Peat, organic material	5.34	±0	−25	5.47	Paralic swamp, thin peat layer (8 cm thick)	5985; 5761	4036; 3812
PAL 2/6	*C. glaucum,* articulated specimen	3.61	+50	±0	3.36	Shallow lagoon	5903; 5752	3953; 3802*
PAL 2/7	*C. glaucum*, fragment	3.99	+50	−50	3.99	Transitional shallow lagoon to back beach environment	6176; 5997	4226; 4047*
PAL 2/10	*C. glaucum*, fragment	5.43	+50	−50	5.43	Transitional shallow lagoon to back beach environment	7005–6887	5055–4937*
PAL 2/14	*Cerastoderma glaucum*, fragm.	7.51	+50	−100	7.76	Back beach (swamp) environment	7569–7484	5619–5534*
PAL 2/15	*Cerithium vulgatum*	7.86	+100	−50	7.61	Transitional lagoon to back beach (swamp) environment	7660–7590	5710–5640*
PAL 2/21	*C. glaucum*, single valve	10.24	+100	±0	9.74	Lagoon	7836–7746	5886–5796*
PAL 2/26	Wood fragment	11.95	+100	±0	11.45	Lagoon	8101; 7949	6151; 5999
PAL 8/11	Wood fragment	4.52	+50	−50	4.52	Shallow marine, littoral	6398; 6307	4448; 4357
PAL 8/22 PR	Wood fragment	9.86	+50	±0	9.61	Lagoon, transgressive sequence	7937; 7837	5987; 5887
P 11#	Peat, organic material	3.50	±0	−50	3.75	Paralic swamp, basal peat layer	7414; 7022	5465; 5073
P 15#	Peat, organic material	2.00	±0	−50	2.25	Paralic swamp, basal peat layer	3063–2858	1114–909

The upper and lower limits of a palaeo sea level band are given with respect to the sampling depth. Both position and uncertainty range of palaeo sea level bands depend on the quality of the sea level indicators and the sedimentary context in which the samples were deposited.

Note: *C. glaucum—Cerastoderma glaucum*; *D. exoleta—Dosinia exoleta*; *T. planate—Tellina planata*; fragm.—fragment. Further explanations see Table 1.

4.1. The Boukka coastal plain

The new RSL curve for the Boukka coastal plain is based on six sedimentological sea level markers (Fig. 3). Samples BOU 4/13 PR and BOU 7/18 + M were not incorporated into the sea level reconstruction because of probable reworking; they were found in shallow marine deposits which we believe were deposited in a short-term marine incursion. Sample BOU 1/19 M is assumed to be littorally reworked material. Sample BOU 5/27 + PR yielded an age far too young given its elevation, which is possibly due to contamination during sampling.

Palaeo mean sea level was 11.70 m below present sea level (m b.s.l.) by 5100 cal BC. It rose to 11.00 m b.s.l. by 4400 cal BC and 7.10 m b.s.l. by 2.800 cal BC. RSL was at 5.05 m b.s.l. by 1300 cal BC and at 3.35 m b.s.l. by 600 cal BC and then reached the present level. The Boukka curve shows a quasi-linear progression (Fig. 3). Rates of sea level rise increased from 0.9 m/ka during 5100–4400 cal BC to 2.5 m/ka during 4400–2800 cal BC and to 1.4 m/ka during 2800–1300 cal BC. A high rate (2.4 m/ka) was also found for the time period 1300–600 cal BC. The average rise for the last 2500 or so years was calculated as 1.3 m/ka.

4.2. The Palairos coastal plain

The RSL curve for the Palairos coastal plain results from nine sedimentological and four geoarchaeological sea level indicators (Fig. 4). Samples PAL 2/11 and PAL 2/17 yielded ages considerably older than other samples from comparable depths and have anomalously low $\delta^{13}C$-values (Table 1). Sample PAL 2/3, a fragment of a freshwater gastropod shell, is affected by hardwater and/or reworking effects.

The submerged remains of the so-called 'mole of the Corinthians' are located at the southern entrance to the Sound of Lefkada some 8 km west of the Palairos coastal plain. The upper edge of the highest boulder lies at 1.4 m b.s.l. and the structure is dated to the 7th–5th centuries BC (Murray, 1988, pp. 14ff.). Near Pogonia, at the eastern fringe of the Palairos coastal plain, the ruins of another submerged ancient mole from the 4th to 2nd centuries BC lie at 1.5 m water depth (Murray, 1985). This was confirmed by underwater measurements by means of a differential GPS in 2004. In both cases it is assumed that the upper edges of the moles were at least 0.5 m and at most 1.5 m above the former sea level. Additional evidence comes from the lowest working level of a submerged ancient quarry some 5 km southwest of Pogonia near Variko which is presently at 1.40 m b.s.l. The quarry was in use sometime between Classical and Roman times (Wacker, 1999, pp. 49ff.; Lang, 2004, pers. comm.). It is assumed that the corresponding sea level lay at 2.40–1.65 m b.s.l. considering that the boulders were transported by boat. In addition, remains of a Roman floor mosaic at the shore near Palairos lie at present mean sea level which indicates that the corresponding palaeo mean sea level was 1–2 m lower than today. Close to the Variko quarry, a submerged

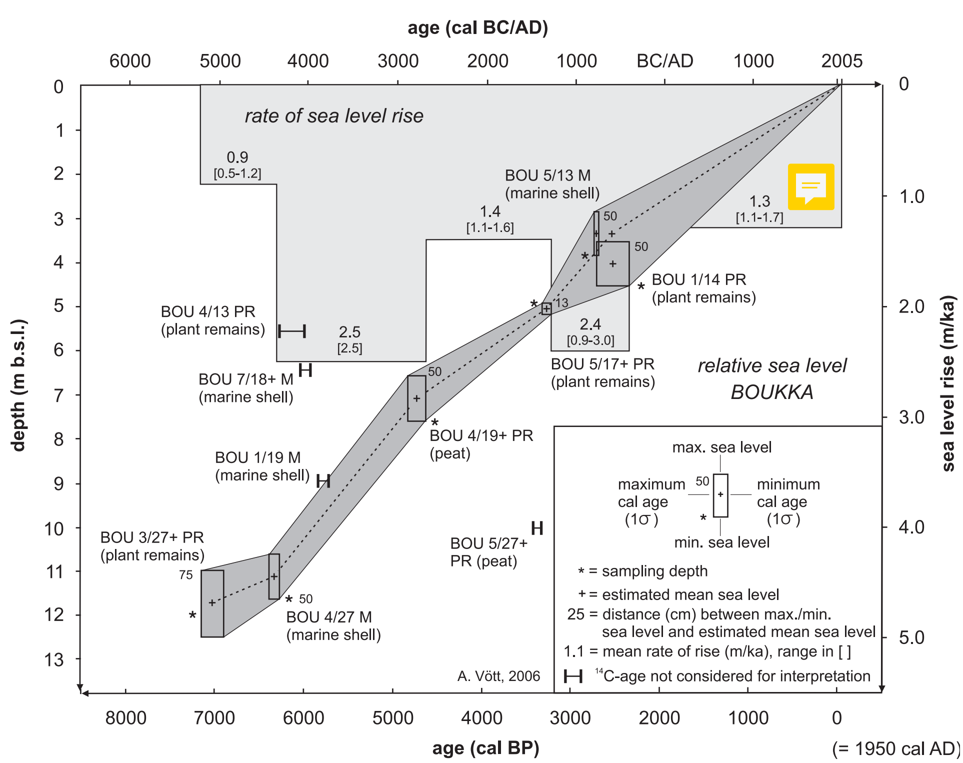

Fig. 3. Relative sea level evolution of the Boukka coastal plain (northern Akarnania, Ambrakian Gulf) since the mid-Holocene and rates of sea level rise. The sea level band is based on radiocarbon dated sedimentological sea level indicators.

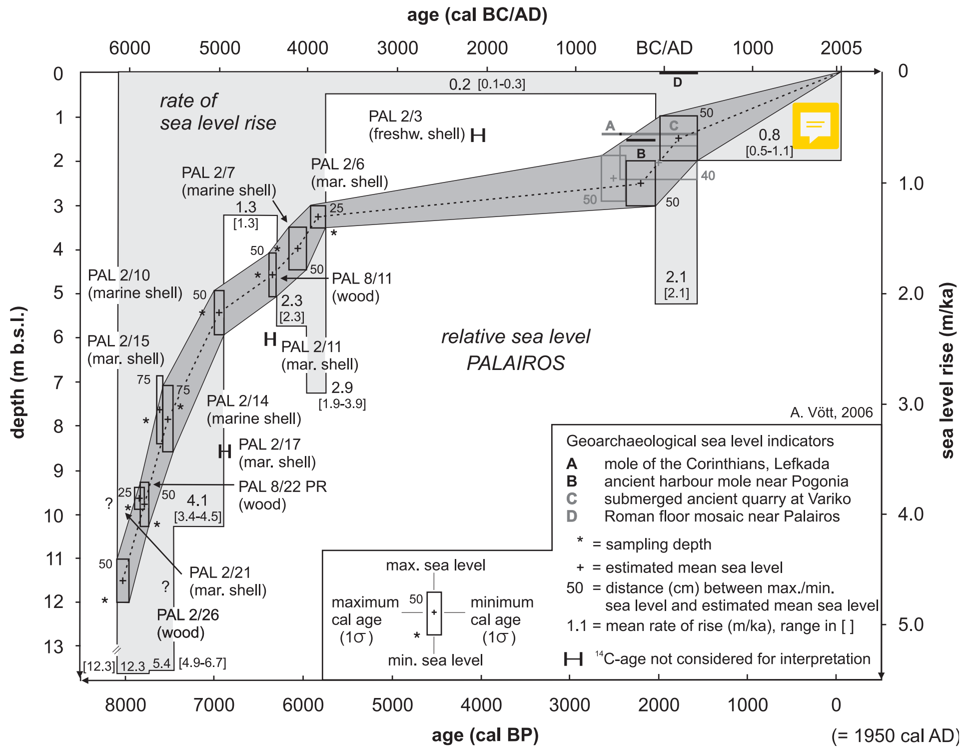

Fig. 4. Relative sea level evolution of the Palairos coastal plain (northwestern Akarnania, Ionian Sea) since the mid-Holocene and rates of sea level rise. The sea level band is based on radiocarbon dated sedimentological and geoarchaeological sea level indicators.

notch occurs at 1.0±0.2 m b.s.l. along a coastal strip, several hundreds of meters long. The notch documents a period of stable sea level after the quarry was flooded. Its pronounced shape indicates that it was drowned during a coseismic event (cf. Pirazzoli et al., 1996).

Palaeo mean sea level stands at Palairos were reconstructed at 11.45 m b.s.l. by 6100 cal BC, at 5.40 m b.s.l. by 5000 cal BC and at 3.25 m b.s.l. by 3900 cal BC. During Classical-Hellenistic times, sea level was at 2.50 m b.s.l. and rose to 1.50 m b.s.l. by 200 cal AD. Sea level rise was strongest during 6100–5000 cal BC and reached values up to 12.3 m/ka. Subsequently, rates decreased to 1.3–2.9 m/ka until 3900 cal BC and then, until 300 cal BC, decelerated to an average of 0.2 m/ka. During 3900–300 cal BC, sea level rise seems to have temporarily stopped or even given way to a slight fall. Since 300 cal BC, it has accelerated anew to 0.8–2.1 m/ka. However, the Variko notch indicates an event of coseismic submergence at some point after Roman times at the latest. All around the Palairos coastal plain, there are no geomorphological markers for a palaeo sea level stand higher than the present one.

4.3. The Mytikas coastal plain

The RSL curve for the Mytikas coastal plain is based on seven sedimentological sea level markers (Fig. 5). The MYT 1/6 freshwater shell radiocarbon analysis was excluded because of the obvious hardwater effect. The plant remains of sample MYT 8/15 PR are embedded in the swampy littoral facies of a coastal lake. They are regarded as in situ with a maximum vertical distance to the palaeo sea level of 50 cm.

Palaeo mean sea level at Mytikas attained 12.35 m b.s.l. by 5900 cal BC, at 9.60 m b.s.l. by 5150 cal BC and at 7.85 m b.s.l. by 4150 cal BC. At 1700 cal BC, RSL reached 5.00 m b.s.l. During antiquity, it rose from 4.15 m b.s.l. by 650 cal BC to 2.30 m b.s.l. at 300 cal AD. Sea level rose quickest during 5550–5150 cal BC with a rate of 4.9 m/ka. Then, rates decelerated to 0.8–1.2 m/ka between 4150 cal BC and 650 cal BC. Since that time, sea level rise has increased to 1.3–2.0 m/ka.

Fig. 6 illustrates facies profiles for a vibracore transect in the Mytikas coastal plain. Sedimentological sea level markers are marked by asterisk. The stratigraphic sequences show good comparability between different vibracores. Mid-Holocene littoral deposits at the bases of MYT 3, 7, 8 and 10 are almost at the same depth indicating negligible or at least identical compaction of mineral deposits. Some of the thin peat layers found in the western part of the plain may even serve as marker horizons as they occur at similar positions and are approximately of the same age. For the upper two sea level markers at MYT 3, peat compaction was estimated as at most 50 cm (Table 2). Palaeogeographical research revealed that the eastern and western fringes of the plain were subject to marine transgression during the past 8000 or so years whereas the profiles from the central plain document regressive sequences for this time period (Vött et al., 2006a).

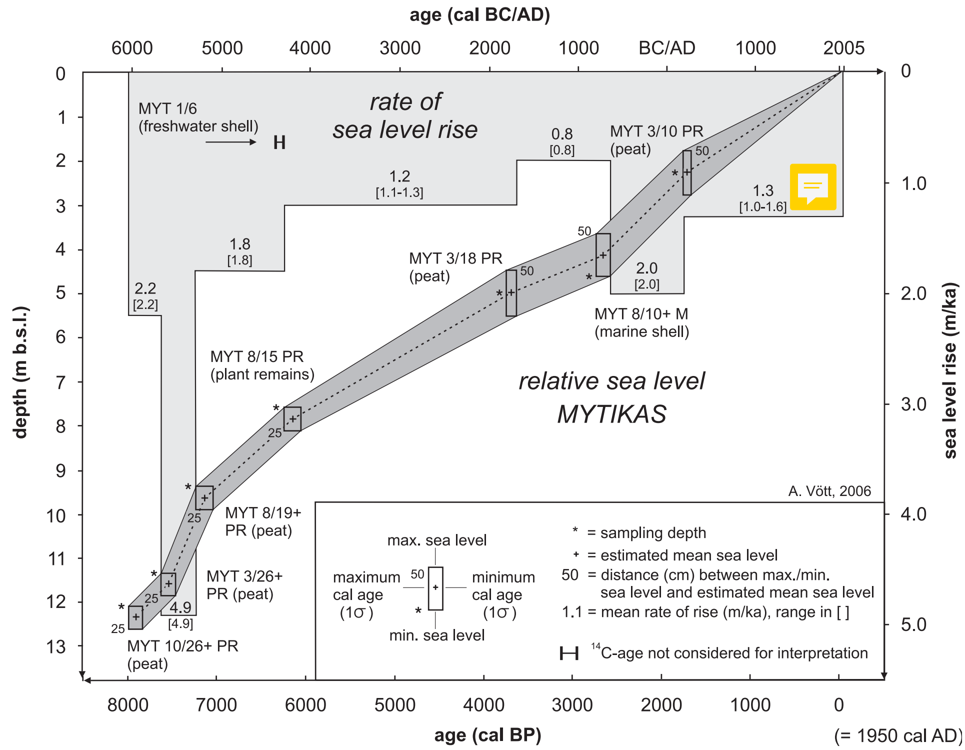

Fig. 5. Relative sea level evolution of the Mytikas coastal plain (western Akarnania, Ionian Sea) since the mid-Holocene and rates of sea level rise. The sea level band is based on radiocarbon dated sedimentological sea level indicators.

4.4. *The Astakos coastal plain*

The reconstruction of RSL fluctuations at Astakos is based on four sedimentological and two geoarchaeological sea level indicators (Fig. 7). Concerning samples AST 2/32 M, AST 1/13 and AST 2/9, sampling depths represent the lower limits for the corresponding palaeo sea levels. The upper limits are given by a 100 cm interval (Table 2). Sample AST 4/42 HK is a less reliable indicator as it was deposited in a limnic setting a few kilometers distant from the former coastline. However, stratigraphic comparisons and time line interpretations let us assume that the corresponding palaeo sea level lay 180–380 cm below sampling depth. The unusual age–depth relation found for sample AST 1/6 indicates it must have been reworked (Vött et al., 2006b). Sample AST 2/23 PR was excluded from further interpretation because of an unusual δ^{13}C-value (Table 1).

Submerged archaeological remains of an early Helladic settlement were found in the Bay of Platiyali some 5 km southeast of Astakos (Delaporta and Spondylis, 1990, p. 128; Delaporta et al., 1990, p. 44; Berkthold, 1996, p. 26). The corresponding palaeo sea level is assumed to lie 100–200 cm below the ruins. In addition, remains of a Roman floor mosaic in the nearby Bay of Pandeleimona (Papageorgiou and Stiros, 1991; Lang, 2005, pers. comm.) document RSL 100–200 cm lower than today. As both the Astakos coastal plain and the archaeological sites of Platiyali and Pandeleimona lie east of the AsFZ, differences in vertical crustal movements are assumed to be of minor importance.

Sea level studies for the Astakos coastal plain show RSL reached 12.55 m b.s.l. by 6150 cal BC, 8.35 m b.s.l. by 5200 cal BC and 6.50 m b.s.l. by 2450 cal BC. Palaeo mean level around 700 cal BC lay at 2.35 m b.s.l. and rose to 1.50 m b.s.l. by 200 cal AD. During 6150–5200 cal BC, the rate of sea level rise reached 4.8–3.0 m/ka. Then, it slowed down to 0.7 m/ka at 5200–2450 cal BC, followed by an increase to 2.4 m/ka during 2450–700 cal BC. Since that time, it has stabilized around 1.0–0.8 m/ka. The sharp inflection in the Astakos curve around 2450 cal BC was probably caused by local coseismic submergence induced by the AsFZ.

4.5. *The Acheloos River delta*

4.5.1. *The Trikardo area*

Eleven peat samples from paralic swamps and one sample from a transgressive unit were used to reconstruct the RSL history of the area around Trikardo (Fig. 8). Sample OIN 55/16+ PR yielded too old an age which may be associated with its abnormally high δ^{13}C-value (Table 1). Samples OIN 1/4 and OIN 6/6 have an anomalous altitude and are derived from cores that were drilled close to the strongly uplifting Kalubitsa mountains and were not incorporated into further analyses. Although the shipsheds of ancient Oiniadai, located in the north of Trikardo (cf. Vött et al., in press a; Vött, in press), are among the best

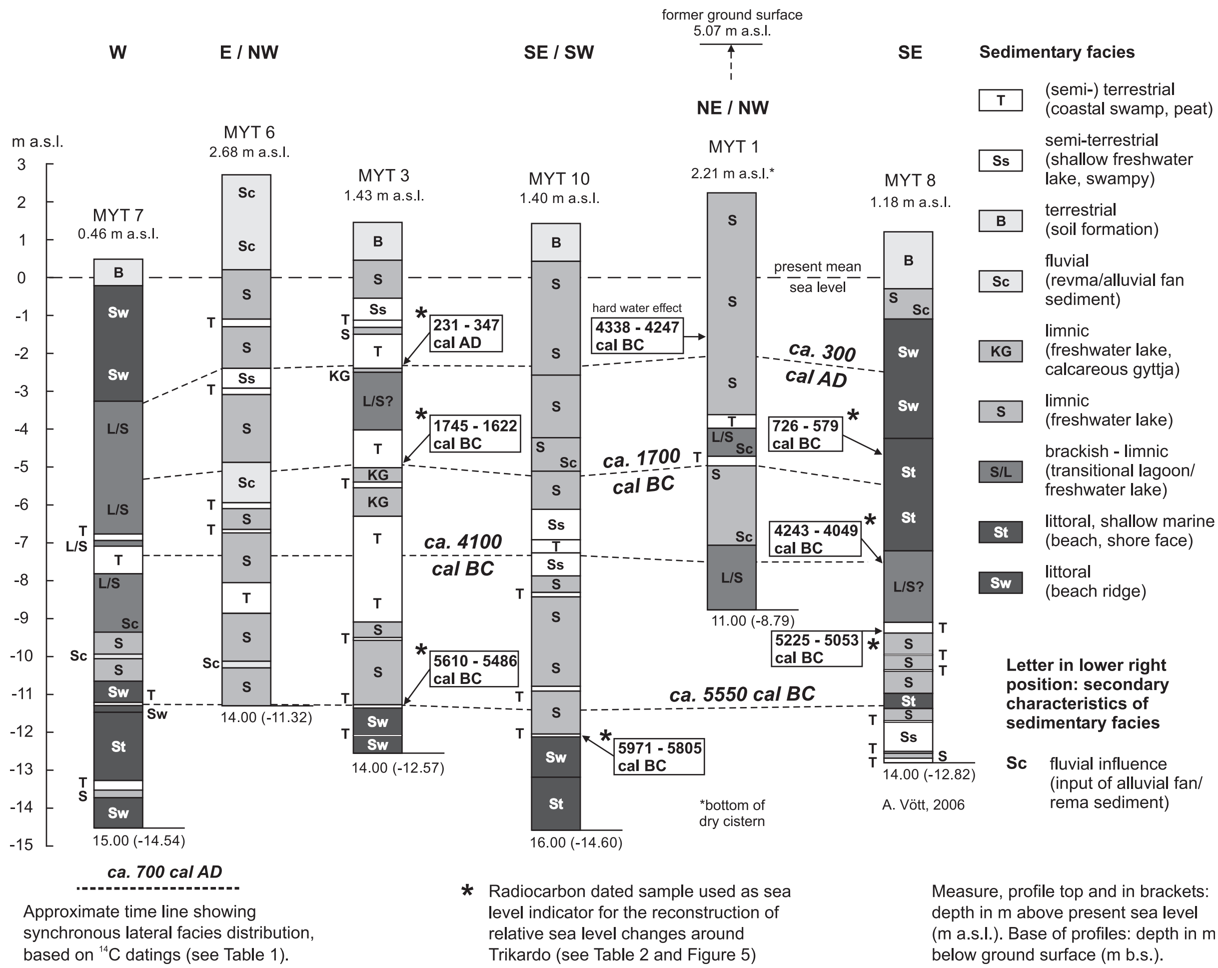

Fig. 6. Vibracore profiles from near-coast geological archives in the Mytikas coastal plain showing vertical sequences of sedimentary environments, stratigraphic relations between cores, and positions of sedimentological sea level indicators. Modified from Vött et al. (2006a).

preserved of their kind in the whole Mediterranean, they do not represent reliable sea level indicators as the lowermost section of the ramps is still uncovered. It is therefore impossible to determine the exact relationship between the slipways and the palaeo sea level.

For the Trikardo area, palaeo mean sea level stands were found at 8.35 m b.s.l. by 5400 cal BC, at 7.30 m b.s.l. by 5100 cal BC and at 6.30 m b.s.l. by 4600 cal BC. Subsequently, sea level rose to 4.65 m b.s.l. by 3100 cal BC and to 3.10 m b.s.l. by 100 cal BC. Around 1400 cal AD, it was still considerably lower than today (1.50 m b.s.l.). The rate of sea level rise was highest during 5400–5100 cal BC reaching 4.0 m/ka. It continuously decreased to a minimum rate of 0.5 m/ka from 2800–100 cal BC before accelerating anew to 0.9 m/ka during 100 cal BC — 1400 cal AD and to 2.7 m/ka since 1400 cal AD. The strong increase around 1400 cal AD is possibly due to coseismic submergence.

Fig. 9 exemplarily illustrates the stratigraphic sequences of three vibracores from the southern embayment of Trikardo and its surroundings. The upper surface of the bedrock clearly decreases towards the south showing that Trikardo was an island in former times. During early to mid-Holocene sea level rise a beach formed at the southern entrance of the bay around OIN 63 and dammed a swamp around OIN 49. This swamp was partly fed by water from adjacent karstic springs. The almost identical position of deltaic sediments encountered in cores OIN 49, 63 and 41 document that sediment compaction until that time was nearly the same at the three sites. Additionally, the thin peat layer dated from the mid-core section of OIN 63 corresponds well to the age–depth relations encountered at OIN 49 and thus indicates that peat compaction in the lower part of OIN 49 seems to be negligible. However, for the upper three sea level markers taken from OIN 49, peat compaction was assumed to be 50–100 cm partly due to anthropogenic groundwater lowering (Table 2). In a palaeogeographical point of view, Fig. 9 documents that in antiquity the southern flank of Trikardo was exposed to a lagoonal environment and no longer to open marine conditions (Vött, in press).

4.5.2. *The environs of the Lagoon of Etoliko*

Seven peat samples are used to reconstruct the RSL curve for the area around Etoliko (Fig. 10). As the geochronological database does not contain local sea level indicators younger than 2550 cal BC, a set of three peat

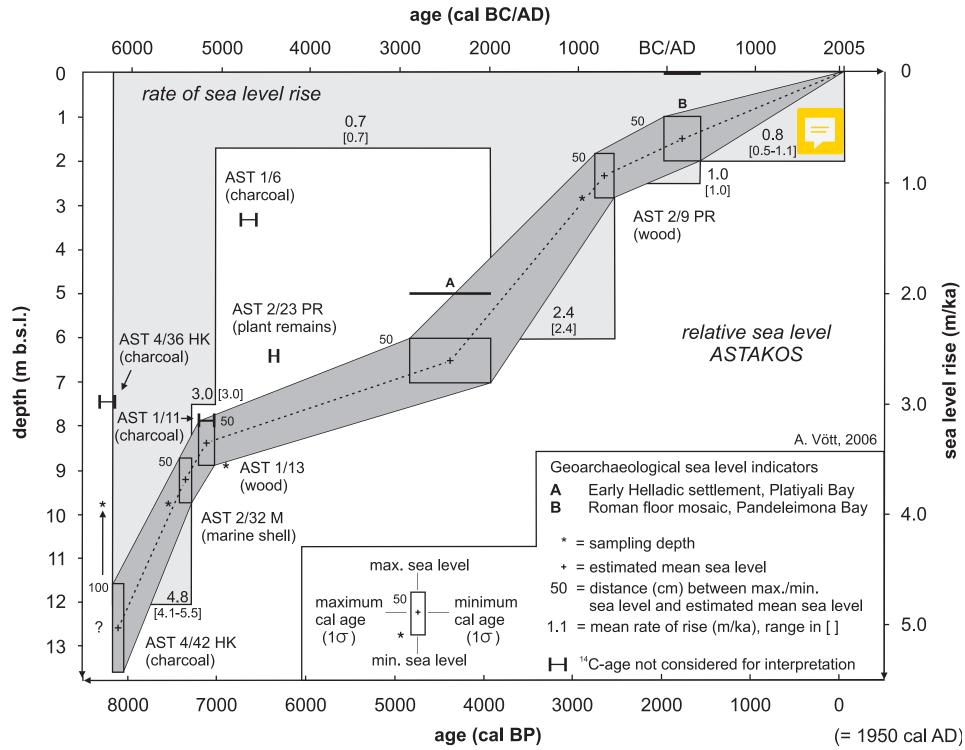

Fig. 7. Relative sea level evolution of the Astakos coastal plain (western Akarnania, Ionian Sea) since the mid-Holocene and rates of sea level rise. The sea level band is based on radiocarbon dated sedimentological and geoarchaeological sea level indicators.

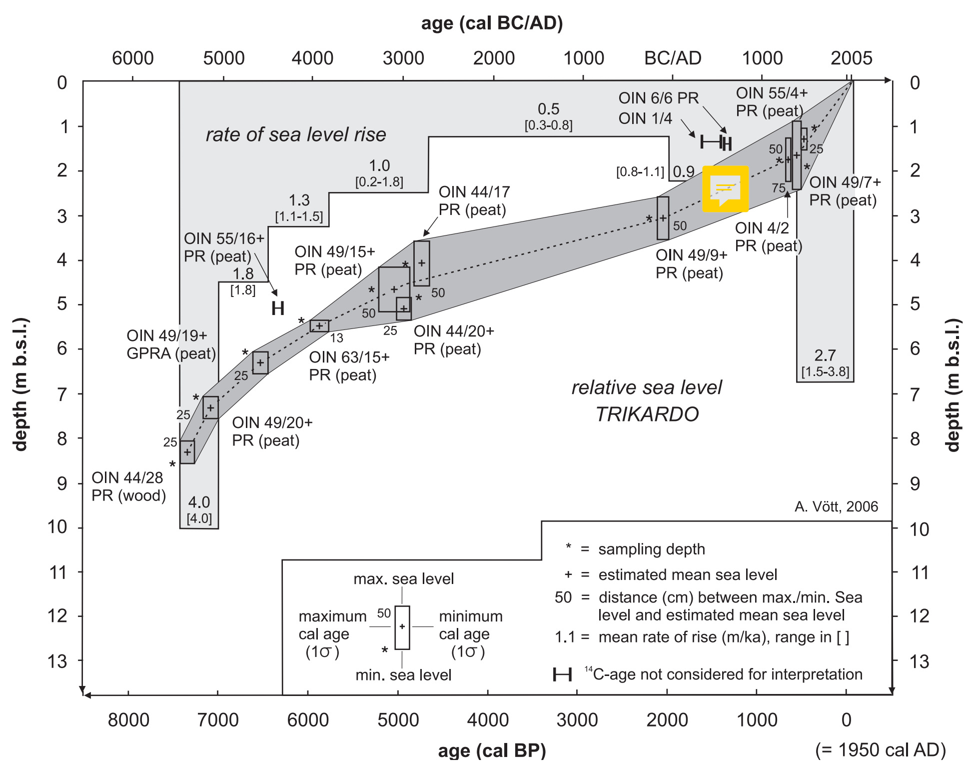

Fig. 8. Relative sea level evolution of the area around the former Echinades Island of Trikardo (Acheloos River delta, southern Akarnania, Ionian Sea) since the mid-Holocene and rates of sea level rise. The sea level band is based on radiocarbon dated sedimentological sea level indicators.

samples (OIN 4/2 PR, OIN 49/7+ PR, OIN 55/4+ PR) from the central Acheloos River delta was incorporated into the analysis.

The palaeo mean sea level was at 12.70 m b.s.l. by 6150 cal BC. It subsequently rose to 9.35 m b.s.l. by 5550 cal BC and 7.90 m b.s.l. by 4750 cal BC. Around

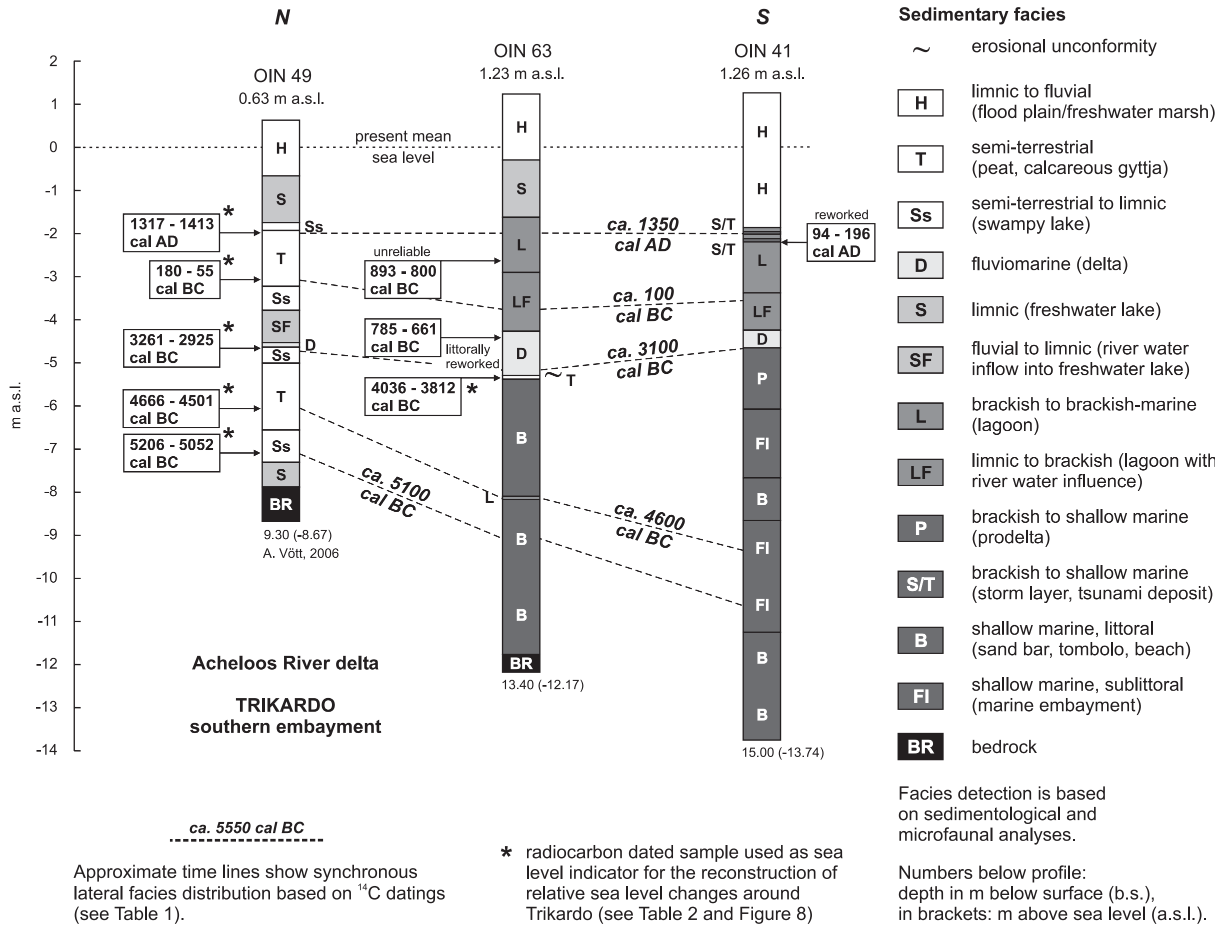

Fig. 9. Facies profiles from geological archives in the environs of the southern embayment of the former Trikardo Island, Acheloos River delta, showing vertical sequences of sedimentary environments, stratigraphic relations between cores, and positions of sedimentological sea level indicators. Modified from Vött (in press).

2550 cal BC, RSL had already reached 3.50 m b.s.l. Similar to the situation around Trikardo, we suggest that around 1400 cal AD the palaeo mean sea level stood at 1.50 m below its present position. The rate of sea level rise shows highest values (5.3 m/ka) at 6150–5550 cal BC, then decreased to 1.9–2.0 m/ka until 2550 cal BC. It seems to have been lowest until 1400 cal AD (0.4 m/ka) and has increased again to 2.7 m/ka during the past 600 or so years.

4.6. The coastal plains of Elis

The RSL curve presented for the Elis coastal plains is based on five sedimentological sea level markers (Fig. 11). Two indicators from cores drilled by Kraft et al. (2005) in the same area were also added to the analysis. The corresponding ^{14}C dates were recalibrated and incorporated into the local geochronological database. Sample P 15 from Kraft et al. (2005) indicates that the palaeo water depth for the ELI 10/9 + PR sea weed remains was around 1.75–2.25 m.

The data presented show that the RSL stood at 4.40 m b.s.l. at 5250 cal BC. It subsequently rose to 3.70 m b.s.l. by 3900 cal BC and to 2.25 m b.s.l. by 1000 cal BC before attaining its present level. The Elis sea level curve is quasi linear with a rate of 0.5 m/ka during 5250–1000 cal BC. Since that time, the value has slightly increased to 0.7 m/ka.

4.7. Relative sea level evolution in Akarnania

In summary, our results document that (i) in all the study areas RSL has never been higher than at present, thus marking the Holocene sea level high stand and (ii) that RSL history since the mid-Holocene shows strong local differences (Fig. 12). Assuming that the eustatic and isostatic sea level components are identical for the whole area, these differences are most readily explained by differences in (a) tectonics, (b) sediment supply and sediment compaction, (c) coastal dynamics and (d) anthropogenic impacts. In general, factor (b) is assumed to have been similar for all the study areas except the Acheloos River delta where sediment supply during the Holocene far exceeds the amounts of sediment which have been transported to the smaller coastal plains by torrential fluvial systems (remata). Moreover, there are no considerable local discrepancies for factors (c) and (d). It is therefore concluded that intra-regional differences in RSL

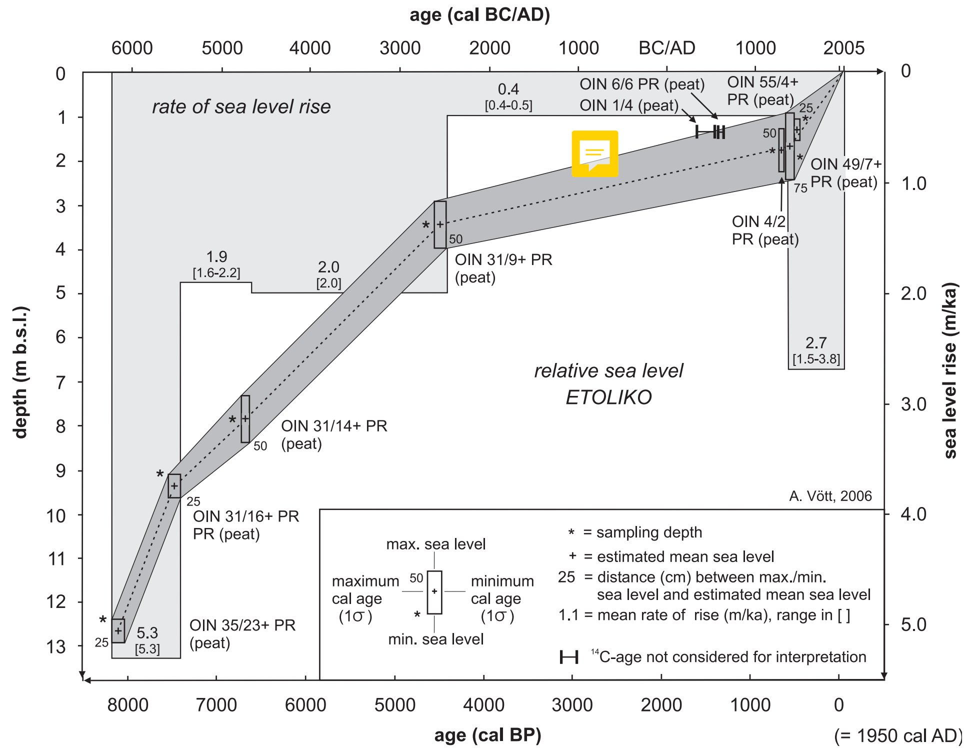

Fig. 10. Relative sea level evolution around Etoliko (Acheloos River delta, southern Akarnania, Ionian Sea) since the mid-Holocene and rates of sea level rise. The sea level band is based on radiocarbon dated sedimentological sea level indicators.

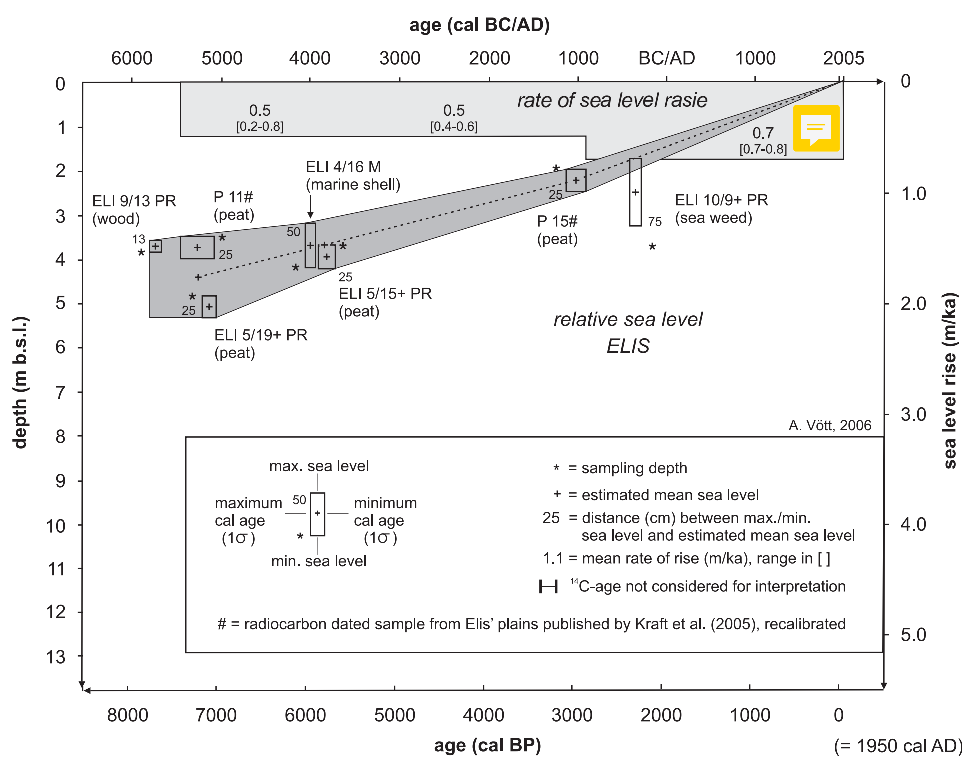

Fig. 11. Relative sea level evolution of the Elis coastal plains (northwestern Peloponnese, Ionian Sea) since the mid-Holocene and rates of sea level rise. The sea level band is based on radiocarbon dated sedimentological sea level indicators.

change (Fig. 12) are mostly due to intra-regional differences in the direction and the rate of tectonic movements as well as in the general activity pattern of local fault systems.

An approximate regional sea level curve for the whole study area is calculated by combining the different records from northwestern Greece (Fig. 12). Calculations were

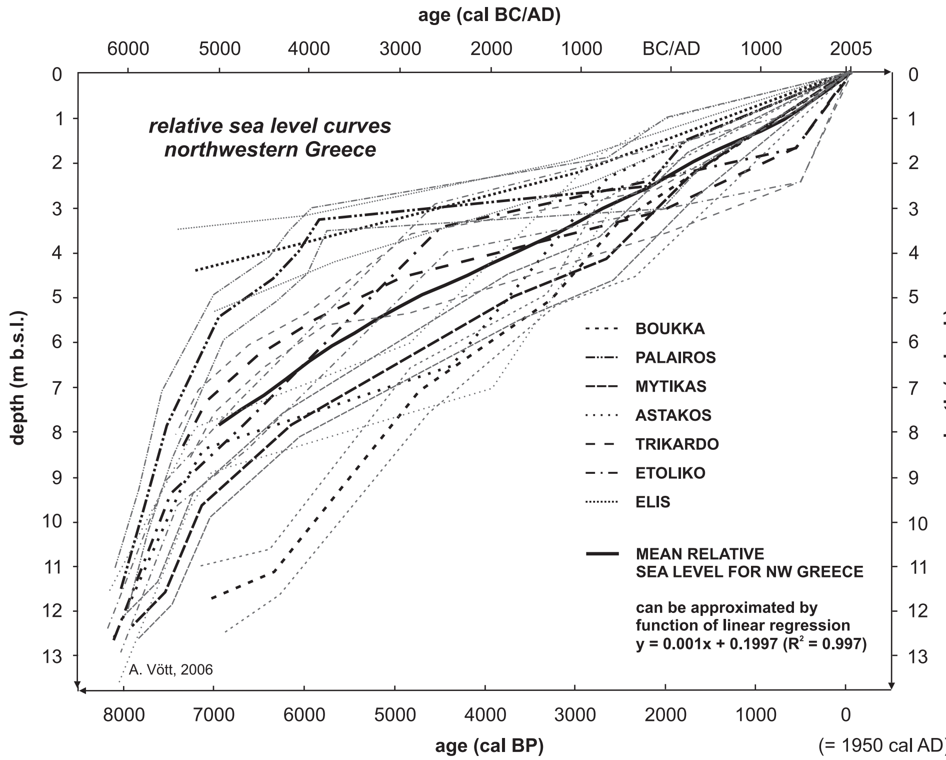

Fig. 12. Summarized view of the relative sea level evolution of seven coastal areas in northwestern Greece. Palaeo mean sea level curves and uncertainty bands are based on sedimentological and geoarchaeological sea level indicators. The mean relative sea level evolution of northwestern Greece was calculated as the average of all relative sea level curves.

based on palaeo mean sea level data reconstructed for each area. The resulting graph indicates a strongly linear trend ($R^2 = 0.997$) with a mean rate of rise of 1.0 m/ka.

5. Regional tectonics evidenced by differences in relative sea level evolution

The RSL history of each study site is now compared with all the other curves found for the region. Differences in the rate of mean sea level change are calculated at 250-year intervals. Following this scheme, each of the comparative curves was substracted from the curve under focus. The calculations are based on mean sea level curves (data given in m b.s.l.) which were derived from sedimentological and geoarchaeological indicators (Figs. 3–5, 7–8, 10–12). It was refrained from determining mathematical approximations for the individual curves in order to stay as close as possible to the original values. Fig. 12 clearly documents that palaeo sea level bands increasingly overlap in the course of the past 3000 or so years. This is mainly due to the fact that all mean curves and bands converge towards the present sea level. Consequently, calculated differences become smaller towards the present. Interpretations thus should take into account the stratigraphic background and further geoarchaeological as well as geomorphological sea level indicators (Sections 6 and 7.1).

In general, the results obtained for the seven coastal areas in northwestern Greece can be grouped into three main types of intra-regional differences. Type 1 shows differences >0, type 2 differences <0 and type 3 comprises all cases with differences ± 0. Each type is presented by a set of curves calculated for a representative study area. Figs. 13–15 can be interpreted by means of a tectonic rhomb. When aligned to the individual curves, the rhomb helps to detect phases of (relative) uplift, subsidence or stability of the area under focus compared to all the other study sites. It shows both the general direction and the intensity of relative tectonic movements.

5.1. Type 1: differences in relative sea level > 0

Comparing RSL data (in m b.s.l.) obtained for the coastal plains of Boukka, Mytikas and Astakos with any other investigated sites in northwestern Greece shows that intra-regional differences are predominantly lower than zero. This indicates prevailing tectonic subsidence of type 1-areas. Fig. 13 exemplarily depicts the results for the Boukka coastal plain.

In a regional context, the Boukka coastal plain is the area which has been most strongly affected by tectonic subsidence during the past 7000 years (Fig. 13). Compared to the plains of Palairos and Mytikas and the areas around Trikardo and Etoliko, the Boukka plain was uplifted at 5000–4000 cal BC. At the same time, subsidence occurred in comparison to the coastal plains of Astakos and Elis. During 4000–500 cal BC, the Boukka plain strongly subsided obviously related to a highly active phase of the AmFZ near Amfilochia. Fig. 13 shows that subsidence of

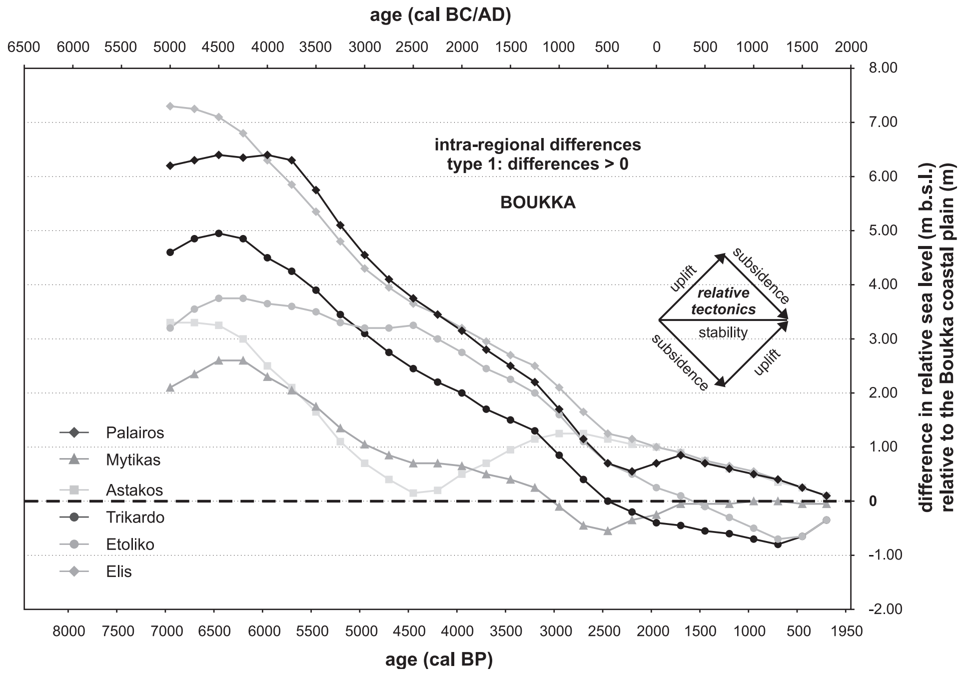

Fig. 13. Intra-regional differences in relative sea level evolution in northwestern Greece: The Boukka coastal plain as example for type 1, differences > 0. Differences were calculated between the Boukka coastal plain and all other study sites in northwestern Greece based on relative sea level data in m below present sea level (m b.s.l.). The rhomb indicates periods of relative subsidence, uplift or stability of the Boukka plain.

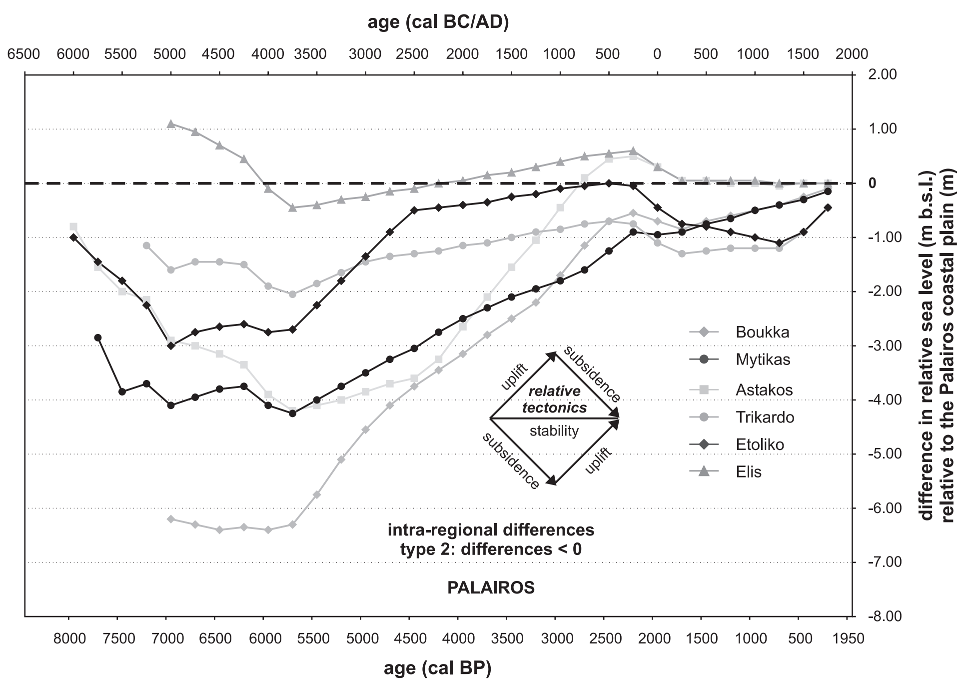

Fig. 14. Intra-regional differences in relative sea level evolution in northwestern Greece: The Palairos coastal plain as example for type 2, differences < 0. Differences were calculated between the Palairos coastal plain and all other study sites in northwestern Greece based on relative sea level data in m below present sea level (m b.s.l.). The rhomb indicates periods of relative subsidence, uplift or stability of the Palairos plain.

the Etoliko area was of almost the same order until 2500 cal BC which indicates that, until that time, the whole AmFZ rift system was active (Fig. 2). During 2500–500 cal BC, however, the Boukka plain was uplifted in comparison to the Astakos area. At 500 cal BC, subsidence relative to the rest of northwestern Greece stopped and the Boukka area became subject to minor uplift until 250 cal AD. At 250–1250 cal AD, a second phase of relative subsidence set in. All over Akarnania, only the Mytikas plain subsided at almost the same rates.

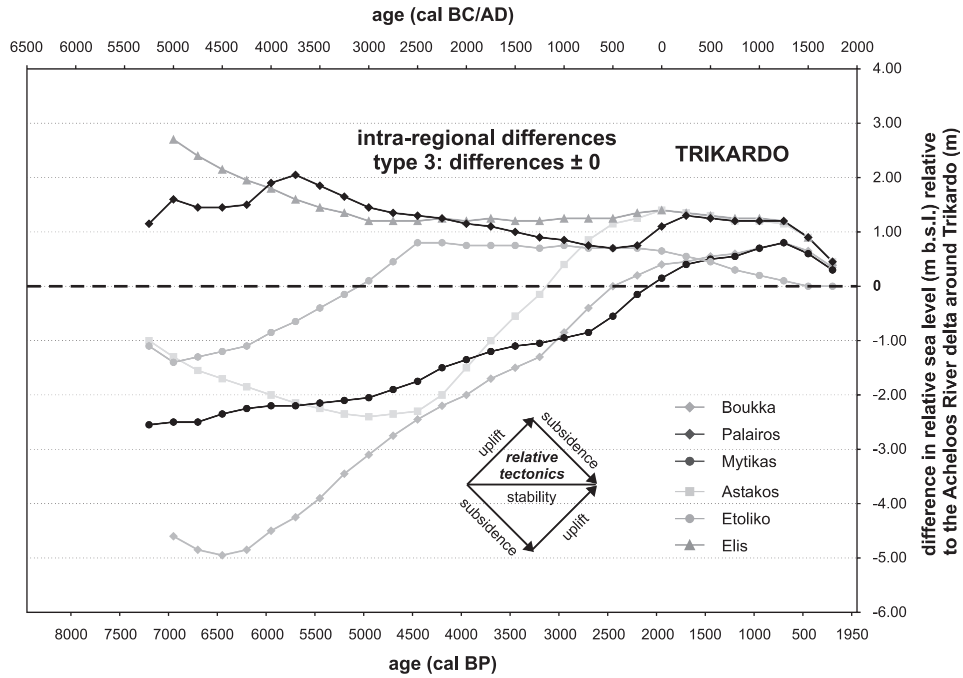

Fig. 15. Intra-regional differences in relative sea level evolution in northwestern Greece: The Trikardo area as example for type 3, differences ±0. Differences were calculated between the Trikardo area and all other study sites in northwestern Greece based on relative sea level data in m below present sea level (m b.s.l.). The rhomb indicates periods of relative subsidence, uplift or stability of the Trikardo area.

Since 1250 cal AD, the Boukka plain has been uplifted compared to the Acheloos River delta, has subsided in comparison to the plains of Palairos, Astakos and Elis, and has remained stable compared to the Mytikas site.

5.2. Type 2: differences in relative sea level < 0

Two of the seven coastal sites investigated in northwestern Greece, the Palairos and the Elis plains, show intra-regional differences mostly greater than zero. This reflects a predominance of coastal uplift within the regional tectonic framework. The curves calculated for the Palairos coastal plain are presented as examples for type 2-areas (Fig. 14).

Strong subsidence of the Palairos plain is recorded at 6000/5000–3750 cal BC with respect to all other study areas. This explains the high extreme rates of RSL rise found for Palairos during that period of time (Figs. 4, 12 and 14). Between 3750 and 250 cal BC, a phase of considerable relative uplift followed. Another change occurred around 250 cal BC when minor subsidence set in and lasted until 250 cal AD. Since that time, the Palairos plain remained almost stable compared to adjacent areas. Relative tectonic movements at Palairos are thus characterized by a sequence of strong subsidence and subsequent major uplift followed by minor fluctuations.

5.3. Type 3: differences in relative sea level ± 0

Trikardo and Etoliko belong to type 3-areas characterized by intra-regional differences which, since the mid-Holocene, show fluctuations around zero. On a regional scale, this means predominant tectonic stability. Fig. 15 illustrates RSL changes at the central Acheloos River delta around Trikardo.

Between 5000 and 2500 cal BC, the Trikardo area subsided relative to Astakos and Elis and partly also to Palairos (Fig. 15). However, the predominant movement in comparison to Boukka, Mytikas and Etoliko was one of uplift. Between 2500 and 250 cal BC, the Trikardo site underwent uplift relative to Boukka, Mytikas and Astakos whereas conditions remained almost stable in comparison to Palairos, Elis and Etoliko. Only little change occurred between 250 cal BC and 1250 cal AD whereas, at 1250 cal AD, the Trikardo area may have experienced a major pulse of subsidence.

6. Multiple regional tectonic events in northwestern Greece

Intra-regional differences of RSL exemplarily shown data were calculated for each study area (Section 5), with average differences determined for each site and different points in time (Fig. 16). The results detail, for each study area, the mean local differences in RSL relative to all other investigated sites (Figs. 12 and 16).

Based on intra-regional differences in RSL for the Boukka (Fig. 13), Palairos (Fig. 14) and the Trikardo areas (Fig. 15) as well as on the mean local differences in RSL evolution (Fig. 16), it can be concluded that, on the regional scale of northwestern Greece, (i) the Boukka, Astakos and Mytikas coastal plains are regions of predominant (relative) subsidence, (ii) the Palairos and

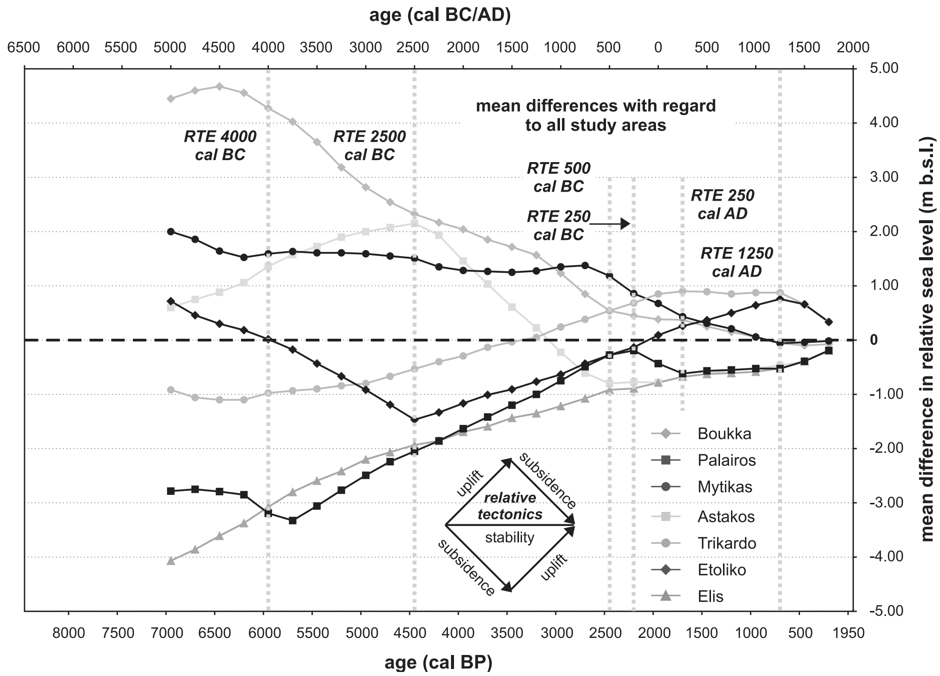

Fig. 16. Mean differences in relative sea level evolution for all study sites in northwestern Greece. Differences are mostly due to differenences in the tectonic activity patterns of local fault systems. Abrupt changes in the progressions of the curves indicate redirection of the tectonic movement or changes in uplift/subsidence rates connected with regional tectonic events (RTEs). RTEs were found for the time around 4000, 2500, 500 and 250 cal BC as well as around 250 and 1250 cal AD. Calculated differences refer to relative sea level data in m below present sea level (m b.s.l.). The rhomb indicates periods of relative subsidence, uplift or stability of each study site. See text for further explanation.

Elis coastal plains are characterized by predominant (relative) uplift and (iii) the Acheloos River delta around Trikardo and Etoliko shows prevailing tectonic stability partially resulting from periods of both (relative) uplift and (relative) subsidence. These three groups correspond to the three different types of relative intra-regional tectonics presented in Section 5.

Most of the curves depicted in Figs. 13–16 reflect a sequence of up- and down-movements. Sharp inflections in the RSL curves mark points in discontinuity of the relative tectonic evolution clustering at several points in time (Fig. 16). It is thus hypothesized that each cluster corresponds to a regional-scale tectonic event. Events are characterized by changes in the direction and the rate of tectonic movements. These changes are not necessarily related to seismo-tectonic activity. Regional tectonic events (RTEs) took place around 4000 cal BC, 2500 cal BC, 500 cal BC, 250 cal BC, 250 cal AD and 1250 cal AD (Figs. 13–16). RTEs thus describe changes in the tectonic movements of the study areas relative to each other. It has to be noted that some sharp bends of the non-averaged curves (Figs. 13–15) were flattened or even disappeared by calculating mean differences (Fig. 16).

The RTE around 4000 cal BC is observed in data from Boukka, Palairos, Mytikas and Trikardo. The RTE around 2500 cal BC caused abrupt shifts in the tectonic dynamics of Astakos and Etoliko as well as slight changes at Boukka and Mytikas. At the same time, Trikardo experienced increased uplift. Another change in regional tectonic dynamics occurred around 500 cal BC inducing deceleration of subsidence at Boukka, acceleration of subsidence at Mytikas and an abrupt stop of subsidence at Astakos. The RTE at 250 cal BC had its largest influence on the Palairos coastal plain and had minor impact on adjacent areas (Fig. 14). However, after the RTE around 250 cal AD, Palairos and Trikardo experienced periods of relative tectonic stability. The youngest RTE took place around 1250 cal AD and initiated relative coastal subsidence in the Acheloos area and relative coastal uplift at Palairos, Astakos and Elis (Fig. 16).

Comparing these results with stratigraphic sequences found for the whole study area, clear relations can be found. Temporary subsidence of the Etoliko area, for example, between 5000 and 2500 cal BC (Fig. 16) seems to have been caused, at least partially, by increased sediment delivery by the Acheloos River. Palaeogeographical studies and earth resistivity measurements reveal that during 4750–1550 cal BC, the Acheloos River delta prograded into the subsiding basin around Etoliko accumulating large quantities of deltaic deposits (Vött et al., in press b). Moreover, geochronological data as well as time line interpretations illustrate that peat formation around Trikardo took place until 4000 cal BC and between around 1 cal AD/BC and 1250 cal AD. Around Mytikas, peat formation stopped completely between around 500 cal BC and 250 cal AD. These data are in good accordance with the general tectonic patterns and the RTEs found for the region (Fig. 16) showing clearly that peat formation at Trikardo and Mytikas is restricted to periods of prevailing tectonic stability.

7. Discussion

7.1. Palaeo sea level research in northwestern Greece

Geological information about Holocene sea level changes in northwestern Greece in literature is limited. In most previous work, estimates of palaeo sea level have been determined from archaeological data. This study represents the first systematic approach to reconstruct sea level changes since the mid-Holocene using a combination of geological and archaeological data.

Jing and Rapp (2003) developed an approximate sea level curve for the area northeast of Preveza based on radiocarbon dated peat samples from gouge auger cores. The curve shows palaeo sea level stands at 5.80 m b.s.l. by 4800 cal BC, at 5.05 m b.s.l. by 3700 cal BC, at 4.35 m b.s.l. by 550 cal BC and at 3.60 m b.s.l. by 450 cal AD (Jing and Rapp, 2003, Fig. 5.20). Poulos et al. (2005) presented a curve for the northern margin of the gulf which was characterized by high-frequency oscillations prior to 2000 BC, but the relationship between sampling depth and the reconstructed RSL are unclear. Kapsimalis et al. (2005, p. 415), interpreting high-resolution seismic analyses and sediment cores from the Ambrakian Gulf, found sea level decelerated and stabilized around 4000 BC. Compared to the Boukka curve presented in this paper (Fig. 3), Jing and Rapp's (2003) data show that the Preveza area was affected by relative uplift until around 1200 cal BC (cf. Brockmüller et al., 2005, p. 47). Subsequently, the RSL history at the two sites have evolved almost identically. These findings independently confirm the results of King et al. (1997, pp. 552ff.) who characterized the Preveza region as an area of major uplift. The strong relative subsidence of the Boukka plain until 1200 cal BC seems to be related to a highly active phase of the AmFZ (Section 5.1).

Pirazzoli et al. (1994a, p. 401) found beachrock slabs up to 1 m a.s.l. along the northern shore of Lefkada Island and interpreted them as indicators for a Holocene sea level highstand. Radiocarbon datings yielded an age interval of 4000–2300 cal BC. Based on recent studies in the Lefkada coastal zone, it has to be assumed that the beachrock plates in question were detached and transported landwards by tsunami impact (Vött et al., 2006d) and therefore cannot be used as sea level markers. In accordance with the newly proposed Palairos sea level curve (Fig. 4), there are no geomorphological indicators along the Palairos–Lefkada coast which document that, during the Holocene, RSL has ever been higher than today (Section 4).

Papageorgiou and Stiros (1991) published an approximate sea level band for the entire Akarnanian coast, based on just four archaeological markers such as the submerged moles at Lefkada and Palairos. In general, the band matches the curves presented for Palairos, Mytikas and Astakos (Figs. 4, 5 and 7). Papageorgiou and Stiros (1991) assumed sudden coastal submergence around 750 AD. This event may be responsible for the submergence of the Variko notch which happened at some point after the nearby Variko quarry had already been abandoned (Section 4.2). Considering the low resolution of the Palairos sea level curve for this period (Figs. 4 and 14), the notch may also have been drowned in the 3rd–5th centuries AD, i.e. during the RTE 250 cal AD. Stiros (2001) found that the 4th to 6th centuries AD represent a period of abnormally high seismicity in the eastern Mediterranean and Pirazzoli (1986) described this interval as the "Early Byzantine Tectonic Paroxysm" (EBTP), a major tectonic event, which occurred around 1530 ± 40 ^{14}C BP. Further research is, however, needed to finally clarify if the submergence of the Variko notch is actually related to the EBTP.

Based on the results presented in this paper it seems that the submergence of the Variko quarry corresponds to the strong increase in RSL found for Palairos around 250 cal BC (Section 5.2, Figs. 12, 14 and 16). This means that the Variko quarry itself was possibly not in use after Classical-Hellenistic times. Comparisons of RSL curves also show that the Palairos area experienced a subsequent phase of predominant stability — conditions that were optimal for the formation of the nearby Variko notch (Section 4.2). Nevertheless, further archaeological research is necessary to get a more accurate age of the Variko quarry. The existence of a submerged notch at Variko as a geomorphological indicator for rapid coastal subsidence does not contradict the fact that the Palairos area represents, on a regional scale, an area of relative uplift within the strongly subsiding Akarnanian region (see Sections 5 and 6, Figs. 16 and 17).

Blackman (1973, p. 128) suggested that sea level during antiquity lay 1.5–2 m lower than today's groundwater level at Oiniadai's shipsheds. According to GPS measurements, this suggests that mean sea level was at 2.20 m b.s.l. for the 5th to 3rd centuries BC which is far too high compared to the 3.25 m b.s.l. sea level reconstructed for the time around 500 cal BC within this study (Fig. 8). Fouache and Dalongeville (2004) even estimated a RSL stand at 1.5 m b.s.l. for the time when the shipsheds were in use. Murray (1982, p. 41), however — based on a vibracoring drilled by Kraft and Villas close to the shipsheds (Villas, 1984) — reconstructed the palaeo sea level at 4.7–5.6 m below ground surface (0.5–1.5 m a.s.l.) which is in broad agreement with the results presented in this paper (Fig. 8).

The RSL curve for Elis (Fig. 11) shows good correspondence with the curve of Kraft et al. (2005) which is based on 10 sedimentological sea level indicators from the area between the Kotiki Lagoon and Lake Kaiafa. Maroukian et al. (2000) report on palaeo sea level stands at 1.2–1.4 m a.s.l. southwest of Kyllini at the Chlemoutsi headland. This region, however, is affected by gypsum diapirism which has led to local coastal uplift of a limited spatial extent (Section 2).

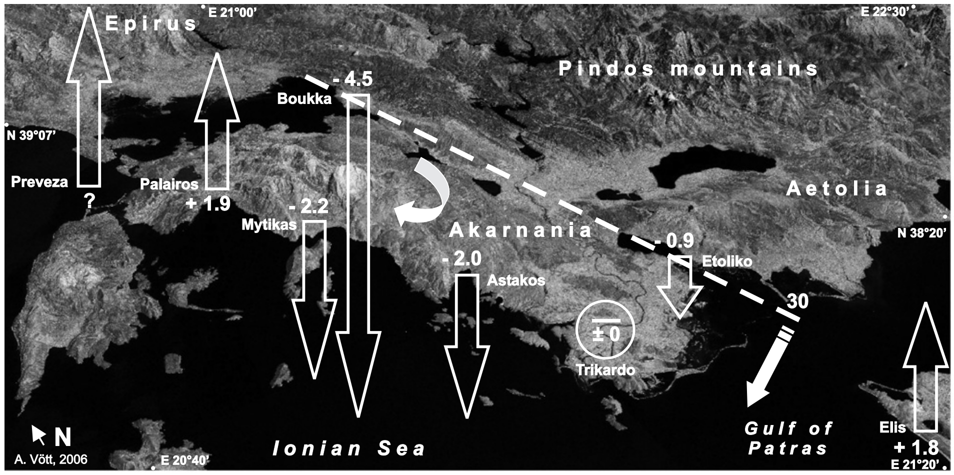

Fig. 17. Relative sea level evolution and (neo-)tectonics of northwestern Greece since the mid-Holocene based on sedimentological and geoarchaeological sea level indicators. Arrows indicate relative vertical movement (m) since 4000 cal BC compared to Trikardo (central Acheloos River delta). As the Akarnanian mass is being separated from central Greece by the rate of 5 mm/a (Cocard et al., 1999), rifting distance since 4000 cal BC is around 30 m. The curved arrow indicates that Akarnania has been rotating in a clockwise direction since Oligo-Miocene times (Broadley et al., 2004, van Hinsbergen et al., 2005). Map based on NASA World Wind 1.3 picture, vertical exaggeration 3 × (access: May 17, 2006).

7.2. Sea level curves for the Eastern Mediterranean sea

RSL rise in northwestern Greece was strongest until 5500–5000 cal BC (up to 12.3 m/ka) due to the influence of ongoing meltwater flux up until this period (e.g. see Kershaw et al., 2005, p. 189). The subsequent deceleration of sea level rise marks decreasing meltwater inflow as an eustatic signal which is known from many sites of the world (cf. Stanley and Warne, 1994; Long, 2001; Figs. 3–5, 7–8, 10–12). Apart from this global structure, the presented RSL curves show essential differences compared to other coastal areas of the eastern Mediterranean.

Based on geomorphological studies in the Peloponnese, Kelletat (1975, 2005a) and Kelletat and Gassert (1975) found a sea level highstand at 3500−3000 BC when the sea reached the present level. A subsequent sea level fall until 1500 BC was followed by a period of rising sea level up to its present position. Similar curves were described by Kayan (1997, Fig. 2) for the coastal area around Troy (western Turkey) and by Wunderlich and Andres (1991) for the western Nile delta. Auriemma et al. (2004) found a relative maximum at 1 m a.s.l. by 5000 cal BC followed by a fall to 3 m b.s.l. by 1500 cal BC on the southern coast of Italy. Müllenhoff (2005, Fig. 47) detected a subordinate sea level maximum at 2.5 m b.s.l. during 2500–2000 cal BC in the Büyük Menderes region (western Turkey). By contrast, the curves presented in this paper do not show interim sea level highstands and subsequent falls, but rather a continuous rise to the present level (Fig. 12), although rates of sea level rise are subject to considerable fluctuations (Section 4).

Using a glacio-hydro-isostatic model and considering earth model parameters, Lambeck (1996, Fig. 4) calculated RSL stands for Greece for the last 18 000 years. For western Greece, sea level is reconstructed at 3 m b.s.l. by 4000 BC and at 1 m b.s.l. by 1 BC/AD. Lambeck and Purcell (2005) as well as Lambeck et al. (2004) adjusted modeling results to palaeo sea level data from geological studies. They found RSL stands at 5.50 m b.s.l. by 4000 BC and at 1 m b.s.l. by 1 BC/AD for the Peloponnese and at 1.35 m b.s.l. during Roman times for the central Mediterranean. The Peloponnese data fit well with the Elis curve depicted in Fig. 11 and the data published by Kraft et al. (2005). Compared to Akarnania, the modeled values are much too low and do obviously not take into account the considerable tectonic subsidence of the area (Fig. 12). Thus, the RSL data presented in this study is regarded as highly useful for adjusting sea level modeling approaches to regions which are strongly affected by tectonics.

Fouache et al. (2005) used ancient harbours and beachrock for the reconstruction of the palaeo sea level evolution along the coast of southern Turkey. However, beachrock slabs south of Alanya, up to 2 m a.s.l., which they interpreted as indicators for a sea level highstand, instead probably represent tsunamigenically dislocated blocks (Kelletat 2005b, pp. 7ff.). Desruelles et al. (2004) dated submerged beachrock along the shores of Mykonos, Delos and Rhenia Islands and found a RSL curve similar to the Palairos and Elis curves (Figs. 4 and 11). This indicates that Akarnania has been subject to coastal subsidence which is partly even stronger than it is known from the Aegean area (Figs. 2, 12 and 17). The latter is part of the back-arc basin to the Hellenic trench and represents a naturally subsiding region. Vouvalidis et al. (2005) developed a sea level curve for the Thermaikos Gulf which shows a slightly convex shape similar to the curves presented in this paper and which documents coastal submergence stronger than that observed for northwestern

Greece (Fig. 12). This might be related to active subsidence connected with the Axios graben.

Modern monitoring approaches, based on satellite altimetry, reveal considerable differences in the short-term sea level evolution for different parts of the Mediterranean Sea. As shown by Cazenave et al. (2002), the Ionian Sea experienced an average sea level fall of 25 mm/a during 1993 and 1998 whereas the Mediterranean Sea as a whole rose by 7 mm/a. This is due to inter-annual to decadal variations in the heat and freshwater budget as well as to changing climatic factors (Zerbini et al., 1996).

In summary, studies all over the eastern Mediterranean suggest that sea level evolution differs strongly from region to region and even — as shown in this paper — on an intra-regional scale. Differences in RSL at a specific point in time are mostly due to tectonic reasons. Thus, RSL curves are a useful instrument to detect inter- as well as intra-regional differences in tectonic activity patterns.

7.3. *Tectonic activity pattern of Akarnania*

The Akarnanian block is moving by an amount of 5 mm/a faster to the SW than the rest of central Greece (Section 2). The results presented in this paper show that the southwestward movement is complemented by strong subsidence of the coastal fringe of Akarnania. As there is no information about crustal subsidence in the more landward parts of Akarnania apart from the narrow AmFZ rift zone (e.g. see Kahle et al., 1995; King et al., 1997; Cocard et al., 1999; Fig. 2) and the flanks of the AmFZ are supposed to be areas of crustal uplift, it is assumed that the Akarnanian block is being tilted or downwarped towards the southwest. However, it could be shown that coastal subsidence is the result of a sequence of up- and down-movements. Moreover, Fig. 16 depicts that the rates of relative subsidence or uplift were not constant over time. This has to be taken into account when considering rates of tectonic movements within the framework of palaeo sea level studies. Similar conclusions were recently drawn by Radtke and Schellmann (2006) based on their analyses of RSL changes at Barbados during the past 500 000 or so years.

Although its coasts are characterized by general subsidence, the tectonic behaviour of the Akarnanian block is quite heterogeneous. Three different subregions can be distinguished (Section 6, Fig. 16). (i) Central Akarnania, including the coastal plains of Mytikas and Astakos as well as the Boukka region, show the highest rates of local subsidence. This is in accordance with results from Clews (1989), King et al. (1997) and Doutsos and Kokkalas (2001). It is concluded that the AmFZ, the AsFZ and the Mytikas faults represent the most active subsiding zones of Akarnania. (ii) The northernmost periphery of Akarnania, the Palairos coastal plain, as well as the coastal plains of Elis show the lowest subsidence rates. Seen on a regional scale, they are characterized by the strongest relative uplift (Fig. 16). This is due to the active emergence of the Preveza zone in the northwest (King et al., 1997) and the strong uplift of the northern part of the Peloponnese in the southeast (Kelletat et al., 1976; Stamatopoulos et al., 1988, 1994; Pirazzoli et al., 2004) both of which reduce the downwarping of the Akarnanian mass at its fringes. (iii) As a result of (i) and (ii), south Akarnania with the Acheloos River delta occupies an intermediate position. The tectonic behaviour of the Trikardo area is, on the one hand, similar to the one found at Elis but shows stronger subsidence. Obviously, this is due to the increased distance to the deceleration moment of the uplifting Peloponnese. Etoliko, on the other hand, lies in the midst of the southern part of the AmFZ (Section 2). During periods of high tectonic activity, such as at 4000–2500 cal BC, it is thus directly affected by subsiding impulses from the AmFZ which exceed the Peloponnese-borne uplift. During the mid-Holocene, subsidence was additionally accelerated by sediment delivery and compaction effects by thick packages of Acheloos River sediments (Vött et al., in press b). Fig. 17 summarizes the differences in the vertical tectonic movements of northwestern Greece since 4000 cal BC found by comparing RSL data. Rates of uplift or subsidence refer to the Acheloos River delta around Trikardo.

For northwestern Greece, several possible RTEs are identified around 4000, 2500, 500 and 250 cal BC as well as around 250 and 1250 cal AD (Sections 5 and 6). Pirazzoli et al. (1994b) reconstructed a sequence of coseismic uplift movements at the Perachora Peninsula at the eastern shore of the Gulf of Corinth, 0.8 ± 0.3 m each, at 5820 ± 60 ^{14}C BP, 4120 ± 60 ^{14}C BP and 1990 ± 100 ^{14}C BP. Calibrating the data and correcting it for a marine reservoir effect of 402 years (Section 3) yields 4344–4229 cal BC, 2321–2133 cal BC and 275–519 cal AD as ages for the tectonic events. This corresponds well to the RTEs at 4000 and 2500 cal BC as well as to the RTE at 250 cal AD of northwestern Greece. Additionally, Stiros (2001) found that the 4th–6th centuries AD were characterized by high-frequency–high magnitude earthquakes (cf. Pirazzoli, 1986, 1988). It was already discussed in Section 7.1 that the RTE around 250 cal AD might be attributed to this period. According to Mastronuzzi and Sansò (2002, p. 603), the southern coast of Italy experienced coseismic uplift at 1231–1389 cal AD which coincides with the RTE at 1250 cal AD of northwestern Greece.

In summary, it seems possible that at least the RTEs at 4000 cal BC, 2500 cal BC, 250 cal AD and 1250 cal AD were related to inter-regional seismo-tectonic events the effects of which are well known from other regions of the eastern Mediterranean. However, further research is needed to solve this question.

8. Conclusions

This paper presents, for the first time, RSL curves for the Holocene for seven coastal areas in northwestern Greece. RSL curves with defined uncertainty margins were reconstructed using sedimentological and geoarchaeological sea level markers of different quality and belonging to different sedimentary environments (Table 2). Palaeo sea level data were used to calculate intra-regional differences in RSL evolution which mostly reflect differences in local tectonics. Our main conclusions are:

(i) Since the mid-Holocene, RSL in Akarnania and the northwestern Peloponnese has never been higher than at present. However, RSL curves for the individual areas show considerable differences (Figs. 3–5, 7–8, 10–12).

(ii) RSL rise was fastest until 5500–5000 cal BC (up to 12.3 m/ka). Shortly afterwards, it decreased to minimum rates during 4000–500 cal BC (0.2–1.4 m/ka; Figs. 3–5, 7–8, 10–12). Since around 500 cal BC, RSL rise has accelerated anew. Local rates strongly differ ranging from 0.7 to 2.7 m/ka.

(iii) The mean trend in RSL of the whole area can be approximated by a strongly linear trend with an average rate of sea level rise of 1.0 m/ka (Fig. 12).

(iv) Compared to other study areas in the eastern Mediterranean, northwestern Greece is characterized by predominant tectonic subsidence (Section 7.2).

(v) Intra-regional differences in RSL were calculated for each study site in order to get information about relative differences in the tectonic behaviour of different parts of northwestern Greece (Figs. 13–15). Further triggers of RSL changes such as sediment loading by the Acheloos River are of minor importance. On a regional scale, the coastal plains of Palairos and Elis are characterized by relative uplift, whereas the Boukka, Mytikas and Astakos plains have strongly subsided since the mid-Holocene. Although the Trikardo and Etoliko areas in the Acheloos River delta underwent minor relative up- and down-movements, they remained comparatively stable.

(vi) In most cases, local sea level evolution shows a sequence of up- and down-movements with a general rising trend. RTEs, indicated by changes in the direction and the rate of relative tectonic movements, were detected for the time around 4000, 2500, 500 and 250 cal BC as well as around 250 and 1250 cal AD. RTEs were possibly related to seismo-tectonic activities along local fault systems (Figs. 2 and 16). Further research will have to show whether some of the RTEs found for northwestern Greece are connected with inter-RTEs which affected larger parts of the eastern Mediterranean.

(vii) The results presented show that the Akarnanian block, being detached from central Greece along the AmFZ, is clearly subsiding at its southwestern fringe. Subsidence is strongest in central Akarnania and lowest in lateral positions where the Preveza area and the northern Peloponnese, both uplifting, act as a deceleration moment (Fig. 17).

Acknowledgements

Sincere thanks are due to the research team at the Faculty of Geography for various support and discussion, especially to H. Brückner, A. Schriever, M. May and S. Brockmüller. I acknowledge fruitful discussion with I. Fountoulis, K. Gaki-Papanastassiou, I. Mariolakos, H. Maroukian, D. Papanastassiou (Athens), D. Kelletat (Essen) and J.C. Kraft (Delaware) about tectonics and sea level changes. L. Kolonas (Athens) and M. Stravropoulou (Mesolongion) kindly supported the team during field work. Work permits were issued by the Greek Institute of Geology and Mineral Exploration (Athens). K. van der Borg (Utrecht) and A. Scharf (Erlangen) carried out radiocarbon dating. Microfauna was analysed by M. Handl (Marburg). Thanks are also due to an anonymous reviewer and to Steve Kershaw (Uxbridge) for valuable comments on an earlier version of the paper as well as to M. Besonen (Amherst) and J. Strube (Marburg) for helpful discussion and correcting my English. I gratefully acknowledge funding by the German Research Foundation (DFG, Bonn, VO 938/1-3).

References

Auriemma, R., Mastronuzzi, G., Sansò, P., 2004. Middle to Late Holocene relative sea-level changes recorded an the coast of Abulia (Italy). Géomorphologie: Relief, Processus, Environnement 1, 19–34.

Behre, K.-E., 2003. Eine neue Meeresspiegelkurve für die südliche Nordsee. Transgressionen und Regressionen in den letzten 10.000 Jahren. Probleme der Küstenforschung im südlichen Nordseegebiet 28, 9–63.

Berkthold, P., 1996. Das prähistorische Akarnanien: Vom Paläolithikum zur geometrischen Zeit. In: Berkthold, P., Schmid, J., Wacker, C. (Eds.), Akarnanien. Eine Landschaft im antiken Griechenland. Herausgegeben von der Oberhummer-Gesellschaft e.V. München, Ergon, Würzburg, pp. 21–59.

Blackman, D.J., 1973. Evidence of sea level change in ancient harbours and coastal installations. In: Blackman, D.J. (Ed.), Marine Archaeology. Butterworths, London, pp. 115–139.

Bousquet, B., 1976. La Grèce occidentale. Interprétation géomorphologique de l'Epire, de l'Acarnanie et des îles Ioniennes. Thesis Université de Paris Sorbonne. Atelier de reproduction des thèses de Lille III, Honore Champion, Paris.

British Petroleum Co. Ltd., 1971. The geological results of petroleum exploration in western Greece. In: Institute for Geology and Subsurface Research (IGSR), Athens (Ed.), The Geology of Greece, Athens, vol. 10, pp. 1–73.

Broadley, L., Platzman, E., Platt, J., Matthews, S., 2004. Palaeomagnetism and tectonic evolution of the Ionian thrust belt, NW Greece. In: Chatzipetros, A., Pavlides, S. (Eds.), Proceedings of the 5th International Symposium Eastern Mediterranean Geology, 14–20 April 2004, Thessaloniki. Extended Abstracts Volume plus CD-ROM, Thessaloniki, vol. II, pp. 973–976.

Brockmüller, S., Vött, A., Brückner, H., Handl, M., Schriever, A., 2005. Die holozäne Entwicklung der Küstenebene von Boukka am Ambrakischen Golf (Nordwestgriechenland). In: Beck, N. (Ed.), Neue Ergebnisse der Meeres- und Küstenforschung. Schriften des Arbeitskreises. Landes- und Volkskunde Koblenz, vol. 4, pp. 34–50.

Brunetti, A., Denèfle, M., Fontugne, M., Hatté, C., Pirazzoli, P.A., 1998. Sea-level and subsidence data from a Late Holocene back-barrier lagoon (Valle Standiana, Ravenna, Italy). Marine Geology 150, 29–37.

Cazenave, A., Bonnefond, P., Mercier, F., Dominh, K., Toumazou, V., 2002. Sea level variations in the Mediterranean Sea and Black Sea from satellite altimetry and tide gauges. Global Planet Change 34, 59–86.

Clews, J.E., 1989. Structural controls on basin evolution: Neogene to Quaternary of the Ionian zone, western Greece. Journal of Geological Society of London 146, 447–457.

Cocard, M., Kahle, H.-G., Peter, Y., Geiger, A., Veis, G., Felekis, S., Paradissis, D., Billiris, H., 1999. New constraints on the rapid crustal motion of the Aegean region: recent results inferred from GPS measurements (1993–1998) across the West Hellenic Arc, Greece. Earth and Planetary Science Letters 172, 39–47.

Delaporta, A., Spondylis, I., 1990. Un habitat Helladique Ancien II à Platiyali Astakou. In: Tzalas, H.E. (Ed.), Proceedings of the 2nd International Symposium. Ship Construction in Antiquity, 27–29 August 1987, Delphi, pp. 127–134.

Delaporta, A., Spondilis, E., Baxevanakis, Y., 1990. Platiyali-Astakos: a submerged Early Helladic site in Akarnania. Enalia Annual 1, 44–46.

Desruelles, S., Fouache, E., Pavlopoulos, K., Dalongeville, R., Peulvast, J.-P., Coquinot, Y., Potdevin, J.-L., 2004. Beachrock and recent sea-level changes on Mykonos, Delos and Rhenia Islands (Cyclades, Greece). Gémorphologie: relief, processus, environnement 1, 5–18.

Doutsos, T., Kokkalas, S., 2001. Stress and deformation patterns in the Aegean region. Journal of Structural Geology 23, 455–472.

Doutsos, T., Kontopoulos, N., Frydas, D., 1987. Neotectonic evolution of northwestern-continental Greece. Geologische Rundschau 76, 433–450.

Einsele, G., 2000. Sedimentary Basins. Evolution, Facies, and Sediment Budget. Second, completely revised and enlarged edition. Springer, Berlin, Heidelberg, New York.

Fairbanks, R.G., 1989. A 17,000 year glacio-eustatic sea level record: Influence of glacial melting rates an the Younger Dryas event and deep ocean circulation. Nature 342, 637–642.

Fouache, E., Dalongeville, R., 2004. Neotectonic impact on relative sea-level fluctuations over the past 6000 years: examples from Croatia, Grecce and Southern Turkey. CIESM (Commission Internationale pour l'Exploration Scientifique de la mer Méditerranée) Workshop Monographs 24, 43–50.

Fouache, E., Sibella, P., Dalongeville, R., 2005. Harbours and Holocene variations of the shoreline between Andriake and Alanya (Turkey). Méditerranée 1 (2), 87–94.

Gehrels, R.W., 1999. Middle and late Holocene sea-level changes in eastern Maine reconstructed from foraminiferal saltmarsh stratigraphy and AMS ^{14}C dates on basal peat. Quaternary Research 52, 350–359.

Geyh, M.A., 2005. Handbuch der physikalischen und chemischen Altersbestimmung. Wissenschaftliche Buchgesellschaft, Darmstadt.

Haslinger, F., Kissling, E., Ansorge, J., Hatzfeld, D., Papadimitriou, E., Karakostas, V., Makropoulos, K., Kahle, H.-G., Peter, Y., 1999. 3D crustal structure from local earthquake tomography around the Gulf of Arta (Ionian region, NW Greece). Tectonophysics 304, 201–218.

Institute of Geology and Mineral Exploration, IGME, 1977. Geological map of Greece, 1:50,000, Neo Manolas Sheet. Athens.

Institute of Geology and Mineral Exploration, IGME, 1986. Geological map of Greece, 1:50,000, Astakos Sheet. Athens.

Jacobshagen, V., 1986. Bau und Entwicklung der griechischen Gebirge. Westgriechenland und Peloponnes. In: Jacobshagen, V. (Ed.), Geologie von Griechenland. Beiträge zur regionalen Geologie der Erde, vol. 19. Berlin, Stuttgart, pp. 11–53.

Jing, Z., Rapp, G. (Rip), 2003. The coastal evolution of the Ambracian embayment and its relationship to archaeological settings. In: Wiseman, J., Zachos, K., (Eds.), Landscape Archaeology in Southern Epirus, Greece I. The American School of Classical Studies at Athens, Hesperia Suppl. vol. 12, pp. 157–198.

Kahle, H.-G., Müller, M.V., Mueller, St., Veis, G., 1993. The Kephalonia transform fault and the rotation of the Apulian Platform: evidence from satellite geodesy. Geophysical Research Letters 20/8, 651–654.

Kahle, H.-G., Müller, M.V., Geiger, A., Danuser, G., Mueller, St., Veis, G., Billiris, H., G. Paradissis, G., 1995. The strain field in NW Greece and the Ionian Islands: results inferred from GPS measurements. Tectonophysics 249, 41–52.

Kapsimalis, V., Pavlakis, P., Poulos, S.E., Alexandri, S., Tziavos, C., Sioulas, A., Filippas, D., Lykousis, V., 2005. Internal structure and evolution of the Late Qauternary sequence in a shallow embayment: The Amvrakikos Gulf, NW Greece. Marine Geology 222–223, 399–418.

Kayan, I., 1997. Bronze Age Regression and Change of Sedimentation on the Aegean Coastal Plains of Anatolia (Turkey). In: Dalfes, H.N., Kukla, G., Weiss, H. (Eds.), Third Millennium BC Climate Change and Old World Collapse. Springer, Berlin, Heidelberg, pp. 431–450.

Kelletat, D., 1975. Eine eustatische Kurve für das jüngere Holozän, konstruiert nach Zeugnissen früherer Meeresspiegelstände im östlichen Mittelmeergebiet. Neues Jahrbuch für Geologie und Paläontologie Monatshefte 6, 360–374.

Kelletat, D., 2005a. A Holocene sea level curve for the eastern Mediterranean from multiple indicators. Zeitschrift für Geomorphologie N.F. Supplement 137, 1–9.

Kelletat, D., 2005b. Neue Beobachtungen zu Paläo-Tsunami im Mittelmeergebiet: Mallorca und Bucht von Alanya, türkische Südküste. In: Beck, N. (Ed.), Neue Ergebnisse der Meeres- und Küstenforschung. Schriften des Arbeitskreises. Landes- und Volkskunde Koblenz, vol. 4, pp. 1–14.

Kelletat, D., Gassert, D., 1975. Quartärmorphologische Untersuchungen im Küstenraum der Mani-Halbinsel, Peloponnes. Zeitschrift für Geomorphologie N.F. Supplement 22, 8–56.

Kelletat, D., Kowalczyk, G., Schröder, B., Winter, K.P., 1976. A synoptic view on the neotectonic development of Peloponnesian coastal regions. Zeitschrift der Deutschen Geologischen Gesellschaft 127, 447–465.

Kershaw, S., Guo, L., Braga, J.C., 2005. A Holocene coral-algal reef at Mavra Litharia, Gulf of Corinth, Greece: structure, history, and applications in relative sea-level change. Marine Geology 215, 171–192.

King, G., Sturdy, D., Bailey, G., 1997. The tectonic background to the Epirus landscape. In: Bailey, G.N. (Ed.), Klithi: Palaeolithic settlement and Quaternary landscapes in northwest Greece, vol. 2. Klithi in its local and regional setting, Cambridge, pp. 541–558.

Kontopoulos, N., 1990. Late Neogene sedimentation in the Paleros-Pogonia Basin (Western Greece). Neues Jahrbuch für Geologie und Paläontologie Monatshefte 4, 233–247.

Kowalczyk, G., Winter, P.K., 1979. Die geologische Entwicklung der Kyllini-Halbinsel im Neogen und Quartär. Zeitschrift der Deutschen Geologischen Gesellschaft 130, 323–346.

Kraft, J.C., Rapp, G. (Rip), Gifford, J.A., Aschenbrenner, S.E., 2005. Coastal change and archaeological settings in Elis. The American School of Classical Studies at Athens, Hesperia, 74/I, pp. 1–39.

Lambeck, K., 1996. Sea-level change and shoreline evolution in Aegean Greece since the Upper Paleolithic. Antiquity 70, 588–611.

Lambeck, K., Chappell, J., 2001. Sea level change through the last glacial cycle. Science 292, 679–686.

Lambeck, K., Purcell, A., 2005. Sea-level change in the Mediterranean Sea since the LGM: model predictions for tectonically stable areas. Quaternary Science Reviews 24, 1969–1988.

Lambeck, K., Anzidei, M., Antonioli, F., Benini, A., Esposito, A., 2004. Sea level in Roman time in the Central Mediterranean and implications for recent change. Earth and Planetary Science Letters 224, 563–575.

Lekkas, E., Fountoulis, I., Papanikolaou, D., 2000. Intensity distribution and neotectonic macrostructure Pyrgos earthquake data (26 March 1993, Greece). Natural Hazards 21, 19–33.

Long, A., 2001. Mid-Holocene sea-level change and coastal evolution. Progress in Physical Geography 25/3, 399–408.

Long, A.J., Waller, M.P., Stupples, P., 2006. Driving mechanisms of coastal change: Peat compaction and the destruction of late Holocene coastal wetlands. Marine Geology 225, 63–84.

Louvari, E., Kiratzi, A.A., Papazachos, B.C., 1999. The Cephalonia Transform Fault and its extension to western Lefkada Island (Greece). Tectonophysics 308, 223–236.

Maroukian, H., Gaki-Papanastassiou, K., Papanastassiou, D., Palyvos, N., 2000. Geomorphological observations in the coastal zone of Kyllini peninsula, NW Peloponnesus-Greece, and their relation to the seismotectonic regime of the area. Journal of Coastal Research 16/3, 853–863.

Mastronuzzi, G., Sansò, P., 2002. Holocene uplift rates and historical rapid sea level changes at the Gargano promontory, Italy. Journal of Quaternary Science 17/5–6, 593–606.

McClusky, S., Balassanian, S., Barka, A., Demir, C., Ergintav, S., Georgiev, I., Gurkan, O., Hamburger, M., Hurst, K., Kahle, H., Kastens, K., Kekelidze, G., King, R., Kotzev, V., Lenk, O., Mahmoud, S., Mishin, A., Nadariya, M., Ouzounis, A., Paradissis, D., Peter, Y., Prilepin, M., Reilinger, R., Sanli, I., Seeger, H., Tealeb, A., Toksoz, M.N., Veis, G., 2000. Global Positioning System constraints on plate kinematics and dynamics in the eastern Mediterranean and Caucasus. Journal of Geophysical Research Solid Earth V 105/3, 5695–5719.

Müllenhoff, M., 2005. Geoarchäologische, sedimentologische und morphodynamische Untersuchungen im Mündungsgebiet des Büyük Menderes (Mäander), Westtürkei. Marburger Geographische Schriften 141.

Murray, W.M., 1982. The coastal sites of western Akarnania: a topographical-historical survey. Ph.D. Thesis, University of Pennsylvania, USA.

Murray, W.M., 1985. The ancient harbour of Palairos. In: Raban, A. (Ed.), Harbour Archaeology. Proc. First Int. Works. Ancient Mediterranean Harbours. British Archaeological Reports International Series vol. 257, pp. 67–80.

Murray, W.M., 1988. The ancient harbour mole at Leukas, Greece. In: Rabner, A. (Ed.), Archaeology of coastal changes. Proc. First Int. Symp. "Cities on the sea — past and present", 22–29 September 1986, Haifa, Israel. British Archaeology Reports International Series, vol. 404, pp. 101–118.

Papageorgiou, S., Stiros, S., 1991. Paleoenvironmental reconstructions, earthquakes and archaeological investigations in NW Greece. In: Proceedings of the Symposium on the Relations between Archaeology and History in Aitoloakarnania, 21–23 October 1988, Agrinion, pp. 233–241 (in Greek).

Papazachos, C.B., Kiratzi, A.A., 1996. A detailed study of the active crustal deformation in the Aegean and surrounding area. Tectonophysics 253, 129–153.

Peltier, W.R., 2002. On eustatic sea level history: Last Glacial Maximum to Holocene. Quaternary Science Review 21, 377–396.

Perissoratis, C., Conispoliatis, N., 2003. The impacts of sea-level changes during latest Pleistocene and Holocene times on the morphology of the Ionian and Aegean seas (SE Alpine Europe). Marine Geology 196, 145–156.

Pirazzoli, P.A., 1986. The early Byzantine tectonic paroxysm. Zeitschrift für Geomorphologie N.F. Supplement 62, 31–49.

Pirazzoli, P.A., 1988. Sea-level changes and crustal movements in the Hellenic Arc (Greece). The contribution of archaeological and historical data. In: Rabner, A. (Ed.), Archaeology of coastal changes. Proceedings of the First International Symposium "Cities on the Sea — Past and Present", Haifa, Israel, September 22–29, 1986. British Archaeology Reports International Series, vol. 404, pp. 157–184.

Pirazzoli, P.A., 1991. World atlas of Holocene sea-level changes. Elsevier Oceanogr. Ser. 58, Amsterdam, London, New York, Tokyo.

Pirazzoli, P.A., 1996. Sea-level Changes. The Last 20 000 Years. Wiley, Chichester.

Pirazzoli, P.A., 1997. Mobilité verticale des cites méditerranéennes à la fin de l'Holocène: une comparaison entre données de terrain et modélisation isostatique. Bulletin de l'Institut Oceánographique Monaco, Numéro spécial 18, 15–33.

Pirazzoli, P.A., Stiros, S.C., Laborel, J., Laborel-Deguen, F., Arnold, M., Papageorgiou, S., Morhange, C., 1994a. Late-Holocene shoreline changes related to palaeoseismic events in the Ionian Islands, Greece. The Holocene 4/4, 397–405.

Pirazzoli, P.A., Stiros, S.C., Arnold, M., Laborel, J., Laborel-Deguen, F., Papageorgiou, S., 1994b. Episodic uplift deduced from Holocene shorelines in the Perachora Peninsula, Corinth area, Greece. Tectonophysics 229/3–4, 201–209.

Pirazzoli, P., Laborel, J., Stiros, S.C., 1996. Coastal indicators of rapid uplift and subsidence: examples from Crete and other eastern Mediterranean sites. Zeitschrift für Geomorphologie N.F. 102, 21–35.

Pirazzoli, P.A., Stiros, S.C., Fontugne, M., Arnold, M., 2004. Holocene and Quaternary uplift in the central part of the southern coast of the Corinth Gulf (Greece). Marine Geology 212, 35–44.

Poulos, S.E., Kapsimalis, V., Tziavos, C., Pavlakis, P., Leivaditis, G., Collins, M., 2005. Sea-level stands and Holocene geomorphological evolution of the northern deltaic margin of Amvrakikos Gulf (western Greece). Zeitschrift für Geomorphologie N.F. Supplement 137, 125–145.

Radtke, U., Schellmann, G., 2006. Uplift history along the Clermont Nose Traverse on the west coast of Barbados during the last 500,000 years — implications for palaeo-sea level reconstructions. Journal of Coastal Research 22/2, 350–356.

Reimer, P.J., McCormac, F.G., 2002. Marine radiocarbon reservoir corrections for the Mediterranean and Aegean Seas. Radiocarbon 44, 159–166.

Sachpazi, M., Hirn, A., Clément, C., Haslinger, F., Laigle, M., Kissling, E., Charvis, P., Hello, Y., Lépine, J.-C., Sapin, M., Ansorge, J., 2000. Western Hellenic subduction and Cephalonia Transform: local earthquakes and plate transport and strain. Tectonophysics 319/4, 301–319.

Shennan, I., Horton, B., 2002. Holocene land- and sea-level changes in Great Britain. Journal of Quaternary Science 17/5–6, 511–526.

Siani, G., Paterne, M., Arnold, M., Bard, E., Métivier, B., Tisnerat, N., Bassinot, F., 2000. Radiocarbon reservoir ages in the Mediterranean Sea and Black Sea. Radiocarbon 42, 271–280.

Sivan, D., Lambeck, K., Toueg, R., Raban, A., Porath, Y., Shirman, B., 2004. Ancient coastal wells of Caesarea Maritima, Israel, an indicator for relative sea level changes during the last 2000 years. Earth and Planetary Science Letters 222, 315–330.

Stamatopoulos, L., Voltaggio, M., Kontopoulos, N., Cinque, A., La Rocca, S., 1988. $^{230}Th/^{238}U$ dating of corals from Thyrrenian marine deposits of Varda area (north-western Peloponnesus), Greece. Geografia Fisica e Dinamica del Quaternario 11, 99–103.

Stamatopoulos, L., Voltaggio, M., Kontopoulos, N., 1994. $^{230}T/^{238}U$-Dating of corals from Tyrrhenian marine deposits and the Paleogeographic Evolution of the Western Peloponnesus (Greece). Münstersche Forschungen zur Geologie und Paläontologie 76, 345–352.

Stanley, D.J., 1995. A global sea-level curve for the late Quaternary: the impossible dream? Marine Geology 125, 1–6.

Stanley, D.J., Warne, A.G., 1994. Worldwide initiation of Holocene marine deltas by deceleration of sea-level rise. Science 265, 228–230.

Stiros, S.C., 2001. The AD 365 Crete earthquake and possible seismic clustering during the fourth to sixth centuries AD in the Eastern Mediterranean: a review of historical and archaeological data. Journal of Structural Geology 23/2–3, 545–562.

Stocchi, P., Spada, G., Cianetti, S., 2005. Isostatic rebound following the Alpine deglaciation: impact on the sea level variations and vertical movements in the Mediterranean region. Geophysical Journal International 162, 137–147.

Stuiver, M., Reimer, P.J., Reimer, R., 2006. CALIB Radiocarbon Calibration. 〈http://calib.qub.ac.uk/calib〉 [last access: May 08, 2006].

Underhill, J., 1988. Triassic evaporites and Plio-Quaternary diapirism in western Greece. Journal of Geological Society of London 145, 269–282.

van Hinsbergen, D.J.J., Langereis, C.G., Meulenkamp, J.E., 2005. Revision of the timing, magnitude and distribution of Neogene rotations in the western Aegean region. Tectonophysics 396, 1–34.

Villas, C., 1984. The Holocene evolution and environments of deposition of the Acheloos River delta, northwestern Greece. Master thesis, Department of Geology, University of Delaware, USA.

Vött, A., in press. Silting up Oiniadai's harbours (Acheloos River delta, NW Greece) — geoarchaeological implications of late Holocene landscape changes. Géomorphologie: Relief, Processus, Environnement.

Vött, A., Brückner, H., 2006. Versunkene Häfen im Mittelmeerraum. Antike Küstenstädte als Archive für die Kultur- und Umweltforschung. Geographische Rundschau 58/4, 12–21.

Vött, A., Handl, M., Brückner, H., 2002. Rekonstruktion holozäner Umweltbedingungen in Akarnanien (Nordwestgriechenland) mittels Diskriminanzanalyse von geochemischen Daten. Geologica et Palaeontologica 36, 123–147.

Vött, A., Brückner, H., Handl, M., 2003. Holocene environmental changes in coastal Akarnania (northwestern Greece). In: Daschkeit, A., Sterr, H. (Eds.), Aktuelle Ergebnisse der Küstenforschung. Berichte Forschungs- und Technologiezentrum Westküste der Christian-Albrechts-Universität zu Kiel, vol. 28, pp. 117–132.

Vött, A., Brückner, H., Schriever, A., Handl, M., Besonen, M., van der Borg, K., 2004. Holocene coastal evolution around the ancient seaport of Oiniadai, Acheloos alluvial plain, NW Greece. In: Schernewski, G., Dolch, T. (Eds.), Geographie der Meere und Küsten. Coastline Reports, vol. 1, pp. 43–53. Rostock-Warnemünde.

Vött, A., Brückner, H., Handl, M., Schriever, A., 2006a. Holocene palaeogeographies and the geoarchaeological setting of the Mytikas coastal plain (Akarnania, NW Greece). Zeitschrift für Geomorphologie N.F. Supplement 142, 85–108.

Vött, A., Brückner, H., Handl, M., Schriever, A., 2006b. Holocene palaeogeographies of the Astakos coastal plain (Akarnania, NW Greece). Palaeogeography Palaeoclimatology Palaeoecology 239, 126–146.

Vött, A., Brückner, H., Schriever, A., Luther, J., Handl, M., van der Borg, K., 2006c. Holocene palaeogeographies of the Palairos coastal plain (Akarnania, NW Greece) and their geoarchaeological implications. Geoarchaeology 21/7, 649–664.

Vött, A., May, M., Brückner, H., Brockmüller, S., 2006d. Sedimentary evidence of late Holocene tsunami events near Lefkada Island (NW Greece). In: Scheffers, A., Kelletat, D. (Eds.), Tsunamis, hurricanes and neotectonics as driving mechanisms in coastal evolution. Zeitschrift für Geomorphologie N.F. Supplement,146, 139–172.

Vött, A., Schriever, A., Handl, M., Brückner, H., in press a. Holocene palaeogeographies of the central Acheloos River delta (NW Greece) in the vicinity of the ancient seaport Oiniadai. 6th Int. Conf. Geomorph., Sept 7–11, 2005, Zaragoza. Working Group Geoarchaeology. Geodinamica Acta, special issue.

Vött, A., Schriever, A., Handl, M., Brückner, H., in press b. Holocene palaeogeographies of the eastern Acheloos River delta and the Lagoon of Etoliko (NW Greece). Journal of Coastal Research.

Vouvalidis, K.G., Syrides, G.E., Albanis, K.S., 2005. Holocene morphology of the Thessaloniki Bay: Impact of sea level rise. Zeitschrift für Geomorphologie N.F. Supplement 137, 147–158.

Wacker, C., 1999. Palairos — Eine historische Landeskunde der Halbinsel Plagia. Würzburg. Studien zur Geschichte Griechenlands 3.

Wunderlich, J., Andres, W., 1991. Late Pleistocene and Holocene evolution of the western Nile delta and implications for its future development. In: Brückner, H., Radtke, U. (Eds.), Von der Nordsee bis zum Indischen Ozean. Erdkundliches Wissen, vol. 105, pp. 105–120.

Zerbini, S., Plag, H.-P., Baker, T., Becker, M., Billiris, H., Bürki, B., Kahle, H.-G., Marson, I., Pezzoli, L., Richter, B., Romagnoli, C., Sztobryn, M., Tomasi, P., Tsimplis, M., Veis, G., Verrone, G., 1996. Sea level in the Mediterranean: a first step towards separating crustal movements and absolute sea-level variations. Global Planet Change 14, 1–48.